Unfolding Simple Folds from Crease Patterns

Hugo A. Akitaya, Jun Mitani, Yoshihiro Kanamori, and Yukio Fukui

1. Introduction

Traditionally, the folding process of origami was transmitted orally and visually by directly showing the folded paper. However, throughout history, attempts have been made to register instructions of particular origami models. Among all types of "written origami," only two are frequently used by contemporary origami artists. They are commonly referenced as *origami diagrams* and *crease patterns*. Origami diagramming was initially devised by Akira Yoshizawa in the 1950s and 1960s [Robinson 04]. It uses lines and arrows indicating the position of the folds and the movement of the paper, as shown in Figure 3 (top). Each step shows the current state of the paper and some indications on how to obtain the state shown in the next step. Usually, the diagrams show the unfolded paper in the first step and the final model in the last step. In this paper, we will show the paper with one side white and the other gray. Dot-dot-dash lines mark the locations of mountain folds, and dashed lines mark the locations of valley folds.

On the other hand, crease patterns show only one picture, which is the unfolded paper containing the creases left by the folds that define the origami model. An example of a crease pattern can be seen in Figure 1. In this paper, we will show the crease pattern white face up with solid lines marking valley folds and dashed lines marking mountain folds. The importance of the crease pattern grew with the rise of mathematical origami and the new design techniques that allowed origami to reach an incredible level of complexity. The fact that the crease pattern only shows the developed/opened state of the paper makes it difficult for nonexperts to grasp any important information regarding the model. However, it indeed can be more illuminating about the origami structure than the image of the folded shape or even diagrams [Lang 04a]. For this reason, many techniques for origami design give a crease pattern as the output. Usually, when the designer produces a technical design, he or she ends up with a crease pattern but has no clue of how to actually fold the model. In fact, it is very hard to fold a model based on a crease pattern. Besides the fact that there is no apparent folding sequence expressed in it, some crease patterns might not even have a folding sequence at all [Lang 11].

Origami diagrams are composed of steps showing subsequent states of the paper. In general, what differs from one state to another is the execution of a fold. In this work, we consider a *fold* to be the bending of one or more layers of the paper localized in a finite number of straight line segments resulting in a dihedral angle of π or $-\pi$. Let us consider that a fold can be categorized as a *simple fold* or a *complex fold*. A simple fold is a fold along a single line that does not end in any internal point of the paper. A complex fold is

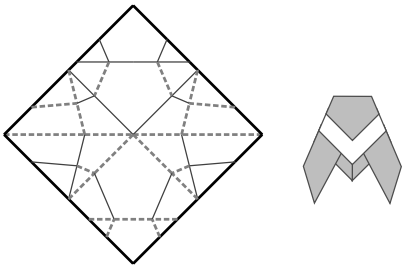

FIGURE 1. Crease pattern (left) and folded form (right) of the traditional cicada origami. Mountain and valley creases are respectively shown as dashed and solid lines.

a combination of folds and unfolds along lines that intersect at internal points. If a crease pattern can be folded with the exclusive use of simple folds, it is called *simply-foldable*.

The paper [Arkin et al. 04] also addressed simple folds. In the authors' models, the paper is only allowed to bend at the creases, and a simple fold causes a rigid movement of the paper around the folding line. The fold is only successful if the movement can be done without unfolding any (already performed) fold and without causing the paper to self-intersect. The authors work with three different models of simple folds: *one-layer*, *some-layers*, and *all-layers*. The one-layer model requires that only one layer is folded at a time. The all-layers model requires that all the layers that are crossed by the folding line are folded simultaneously. The some-layers model supports any number of layers for a given fold. Our model is close to the some-layers model with respect to the number of folded layers, but it is different regarding the general concept of a simple fold. We allow the paper to bend at any place during the fold, making our model closer to what is called *pureland origami* [Smith 80].

Origami designs are usually published in books in the form of origami diagrams. After obtaining a sequence, which is done usually by trial and error, individual drawings that show the folded state of each step have to be drawn. Consequently, diagramming an origami piece is very time consuming. Having this as the motivation, this work aims to produce semi-automatic generated diagrams having a crease pattern as the input. This algorithm was roughly described in [Akitaya et al. 13]. Here, we focus on the theoretical description of simple folds in terms of the crease pattern. Our main contribution is the definition of the minimal set of creases that can be created by a simple fold in a single-vertex origami, which makes possible the identification and the unfolding of any simple fold. With our results, we can determine if a crease pattern of a flat origami is simply-foldable and obtain a folding sequence for it.

2. Background and Related Work

A crease pattern is called *flat-foldable* if it can be flattened in its folded form. Many researchers have investigated the properties of flat origami [Hull 94, Bern and Hayes 96]. We can split the problem of flat-foldability of a crease pattern into local and global. In *local flat-foldability*, we investigate whether the area in the vicinity of a vertex of the crease pattern can be folded flat. *Global flat-foldability* addresses if the origami as a whole can be folded flat, which in general is an NP-hard problem [Bern and Hayes 96].

When checking for local flat-foldability, we consider that each vertex is in the center of a disk of paper and that the paper contains only this vertex. Such a configuration is

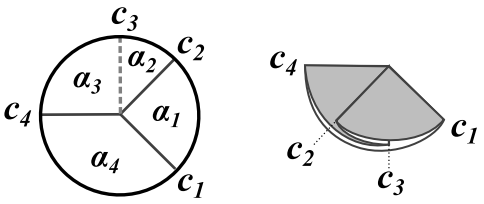

FIGURE 2. Single-vertex origami crease pattern with enumerated creases and angles.

referred to as *single-vertex origami*. A vertex that is located on one of the edges of the paper is called a *border vertex*. All the other vertices are called *internal vertices*. There are three conditions that an internal vertex must obey to be flat-foldable.

Let us consider the single-vertex origami with four creases (c_1, c_2, c_3, c_4) ordered in counterclockwise direction shown in Figure 2. The sequence $(\alpha_1, \alpha_2, \alpha_3, \alpha_4)$ represents the angles around the vertex such that α_i is the angle between c_i and c_{i+1}. The first condition is called *Maekawa's theorem* and states that the number of mountain creases that emanate from the vertex minus the number of valley creases must be either $+2$ or -2. The second condition is called *Kawasaki's theorem* and enunciates that the alternate angles in such a sequence must sum to π. In the example in Figure 2, $\alpha_1 + \alpha_3 = \pi$ and $\alpha_2 + \alpha_4 = \pi$. A consequence of this condition is that the alternating sum of the angles around a vertex must be equal to zero, i.e., $\alpha_1 - \alpha_2 + \alpha_3 - \alpha_4 = 0$. For proofs of both theorems, see [Hull 94].

The third condition was stated by Kawasaki [Kawasaki 91] and enunciates that if $\alpha_i < \alpha_{i-1}$ and $\alpha_i < \alpha_{i+1}$, then, c_i and c_{i+1} must have different mountain/valley assignments. In the example, α_2 is a strict minimum relative to its neighbors and c_2 has opposite assignment to c_3. The proof for this theorem can be found in [Bern and Hayes 96].

The above mentioned conditions are necessary for flat-foldability, but not sufficient. Sufficiency is obtained by a recursive reduction of the crease pattern and application of the third condition, as described in [Demaine and O'Rourke 07]. The third condition must also be followed by the border vertices.

Some origami simulators and diagramming tools have been created. One example is ORIPA, developed by Jun Mitani [Mitani 05]. In addition to the x-ray vision of the folded form, it also obtains the layer ordering. With this information, a rendered image of the folded form is produced. Some simulators try to mimic the interaction between paper and artist in the digital environment. Some examples of this type of approach are the Origami Simulator by Tung Lam [Lam 09] and the Origami Simulation by Robert Lang [Lang 04b]. However, to produce origami diagrams, the user has to already know the folding sequence in advance. Another study investigates simply-foldability in crease patterns containing exclusively orthogonal creases [Arkin et al. 04].

3. Simple Folds

Simple folds, as suggested by the name, are the simplest way to fold a flat configuration of the paper into another flat state. A simple fold always divides the faces where it is applied. Consequently, it will add as many creases to the crease pattern as faces are divided. We assume that simple folds do not unfold any of the pre-existing folds but can only divide them in two, leaving their position and mountain/valley assignment unchanged. Figure 3 shows simple folds applied to one and three layers of paper.

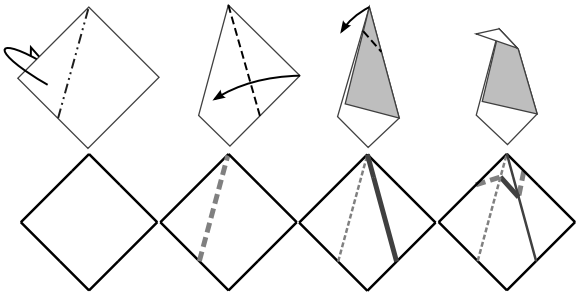

FIGURE 3. How simple folds affect the crease pattern. The corresponding crease pattern of the folded form is shown below each step. Thick lines represents recently added creases.

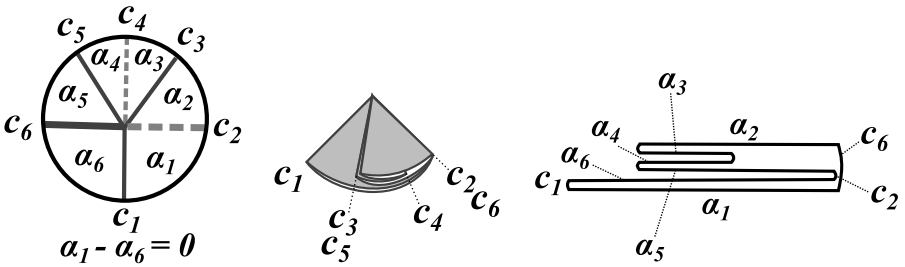

FIGURE 4. (a) Example of reflection creases in a flat-foldable single-vertex origami: c_2 and c_6 are a pair of reflection creases and are shown with thick lines. (b) Folded origami: Creases c_2 and c_6 lie in the same position, as do creases c_3 and c_5. (c) Bottom view of the model with exaggerated thickness.

3.1. Reflection creases. Let us consider a simple fold in a single-vertex origami.

POSTULATE 3.1. *A single-vertex origami must, after the execution of a simple fold, follow the conditions of local flat-foldability.*

A direct consequence of Postulate 3.1 is that, by removing the creases that were added by a simple fold from a flat-foldable single-vertex crease pattern, one would get a flat-foldable crease pattern.

Let us consider two creases c_2 and c_6 shown in Figure 4. The sequence of angles from c_2 to c_6 in counterclockwise direction is $\alpha_2, \alpha_3, \alpha_4, \alpha_5$. Although these creases were created by the same simple fold, the crease pattern shown in Figure 4 is not simply-foldable.

Two creases are folded into the same position if the alternating sum of angles between them is zero. This comes from the fact that a fold bends the paper in the crease region about π or $-\pi$ and can be visualized in Figure 4(c).

DEFINITION 3.2. A pair of creases are called reflection creases of each other, or simply reflection creases, if they have different mountain/valley assignment and the alternating sum of the angles between them add up to zero.

In Figure 4, creases c_2 and c_6 are reflection creases because they have different crease assignments and $\alpha_2 - \alpha_3 + \alpha_4 - \alpha_5 = 0$ and, therefore, $\alpha_1 - \alpha_6 = 0$. The creases of a reflection pair map to folds that coincide when the model is folded. We can observe that if the single-vertex origami is flat-foldable, both clockwise and counterclockwise circling between reflection creases will generate alternate sums that add up to zero. This is a consequence of Kawasaki's theorem. The alternate sum of the whole circumference around the vertex must be zero. Consequently, if the alternate sum from the clockwise direction is zero, the one from the counterclockwise direction will also be zero.

PROPOSITION 3.3. *The removal of a pair of reflection creases from a flat-foldable single-vertex crease pattern generates a new crease pattern that obeys Maekawa's and Kawasaki's theorems.*

PROOF. Since the starting index of the enumeration of creases is arbitrary, to facilitate the notation, let us say that the reflection creases to be removed are c_1 and c_k. Because the creases in the reflection pair have different mountain/valley assignments, if they are removed, the condition of Maekawa's theorem will still be followed. Let the alternate sum of angles around the vertex be $A = (\alpha_1 - \alpha_2 + \alpha_3 - \ldots)$. A can be divided into two terms ($A = A_1 + A_2$) such that A_1 contains the angles from c_1 to c_k and A_1 contains the angles from c_k to c_1 in counterclockwise direction. From the definition of reflection creases, $A_1 = A_2 = 0$. The removal of the pair will cause the fusion of the first/last angle of A_1 with the last/first angle of A_2. The alternate sum for the new vertex (without the creases) will be $A_1 - A_2$, which is also zero. In the example shown in Figure 4, this sum is $(\alpha_1 + \alpha_2) - \alpha_3 + \alpha_4 - (\alpha_5 + \alpha_6) = (\alpha_2 - \alpha_3 + \alpha_4 - \alpha_5) - (\alpha_6 - \alpha_1) = 0$. □

From the proof of Proposition 3.3, we can also conclude that if the removal of a pair of creases produces a crease pattern that obeys the two first conditions of flat-foldability (Maekawa's and Kawasaki's theorems), those creases are a pair of reflection creases.

LEMMA 3.4. *Every simple fold that is performed in a nonempty single-vertex origami adds only pairs (at least one pair) of reflection creases.*

PROOF. A simple fold is performed through a line on the folded model. Every crease that is added by a simple fold must lie in the same position when the pattern is completely folded. Consequently, the alternate sum of angles between the added creases is zero, as previously stated. Considering Postulate 3.1 and Maekawa's theorem, the number of added creases must be even. Each pair of added creases with different assignments is a reflection pair. □

The inverse affirmation, though, is not true; there are reflection pairs that, when removed, produce crease patterns that are not flat-foldable. This is due to the third condition of local flat-foldability described in Section 2.

Lemma 3.4 says that a reflection pair is the minimal unit of creases that can be created by a simple fold in a single-vertex origami.

3.2. Reflection paths. Now that simple folds have been analyzed in a single-vertex origami, this subsection will describe their behavior in multi-vertex origami.

Let a multi-vertex crease pattern be the undirected graph $CP = (V, C)$, where V is the set of vertices and C is the set of creases. Let R_v be the binary relation defined in $C \times C$ such that $c_1 R_v c_2$ is true if c_1 and c_2 are a reflection pair based on the internal vertex $v \in V$.

Definition 3.5. A *reflection path* is a simple walk in CP as $(v_1, c_1, v_2, c_2, \ldots, v_n)$ or a closed walk in which $v_1 = v_n$ such that $c_i R_{v_i} c_{i+1}$ with $i \in [1, n)$. We call this reflection path *maximal* if it is a closed walk or if $\nexists c'$ such that $c' R_{v_1} c_1$ or $c_{n-1} R_{v_n} c'$.

In each crease pattern shown in Figure 3, the highlighted creases form a maximal reflection path.

Lemma 3.6. *The removal of a reflection path affects only its beginning and ending vertices regarding Maekawa's and Kawasaki's theorems.*

Proof. Every internal vertex will have a pair of reflection creases removed when the reflection path is removed. By Lemma 3.3, the conditions of Maekawa's and Kawasaki's theorems will remain unchanged by such vertices. However, at the beginning and ending vertices, only one crease will be removed and the conditions will be altered, in the case of a simple walk. □

From Lemma 3.6 we can also conclude that a reflection path that forms a closed walk produces, if removed, a crease pattern that obeys the first two conditions of flat-foldability. We call a reflection path *complete* if it is a closed walk or if it begins and ends with border vertices.

Theorem 3.7. *The execution of a simple fold can only produce creases that form complete reflection paths.*

Proof. Because border vertices do not have to obey the conditions of Maekawa's and Kawasaki's theorems, the addition or removal of reflection paths that begin and end with border vertices does not affect the first two conditions for flat-foldability at any vertex. If a simple fold adds at least one pair of reflection creases to the vertices it passes through (Lemma 3.4), the combination of these creases will compose reflection paths that have to end/begin at border vertices or form a closed walk. □

A simple fold can add one or more complete reflection paths. Analogous to the single-vertex case, a complete reflection path is the minimal unit of creases that can be created by a simple fold. Consequently, the unfold of a simple fold can be modeled as the removal of the corresponding complete reflection path. However, there may be reflection paths that, when removed, lead to crease patterns that are not flat-foldable due to of self-intersections because the third condition and global flat-foldability are not guaranteed.

4. Results

An implementation of the unfolding method described in this work was made using ORIPA to calculate the folded forms at each step. Notice that the theory described in Section 3 allows us to simplify crease patterns only and not unfold a folded form of the origami. ORIPA also checks the flat-foldability of the model, using a brute-force approach to find valid layer orderings. If a result is not flat-foldable, it can simply be discarded. If more than one folded states are possible (when multiple layer orderings are valid), the user can use an interface similar to ORIPA to choose one of them for the diagrams. The input is a crease pattern in ORIPA file format.

The system checks if there are complete reflection paths. If by removing the path the crease pattern is still flat-foldable, we can unfold a simple fold. If there are more then one complete reflection paths that can be unfolded, there are more than one folding sequences capable of producing the input crease pattern. Figure 5 shows a graph that contains all possible unfolds of an input crease pattern, called a *step sequence graph*.

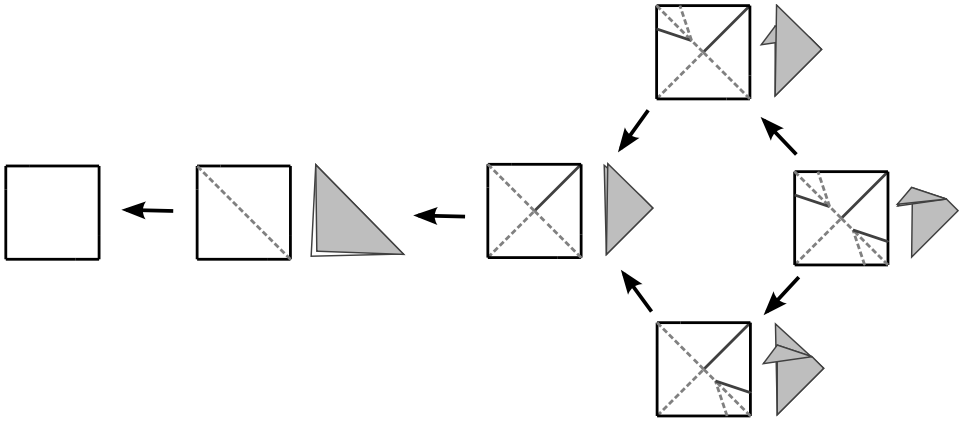

FIGURE 5. A step sequence graph that contains the possible unfoldings of a model.

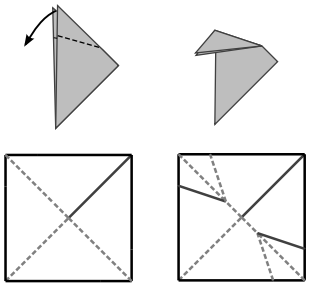

FIGURE 6. A simple fold that folds through many layers of paper and adds more than one complete reflection path to the crease pattern.

Some simple folds can be applied to many layers of paper, as in Figure 6, generating multiple complete reflection paths. Although our method does not produce an unfolding of all the layers at once, the folding sequence shown in Figure 6 is contained in one of the possible generated sequences. Theorem 3.7 assures that our method can unfold any simple fold, by removing the corresponding complete reflection paths.

The user can choose the path in this graph by selecting the desired unfolding and then gradually unfolding the origami until it reaches a square of paper completely developed. The path chosen in this unfolding graph represents an unfolding sequence. By reversing this sequence, we can get a folding sequence. Each crease pattern generates a folded form, using the ORIPA method, and each folded form can be used as a step in an origami diagram. Figure 7 shows diagrams generated by our system. The symbols such as arrows and fold lines were produced automatically by comparing two subsequent steps.

5. Conclusion

In this chapter, a method for the semi-automatic generation of origami diagrams containing simple folds was presented. The proposed method is capable of simplifying gradually the input and generating origami diagrams based on the simplification sequence. The proposed method is capable of generating locally valid flat intermediate states between

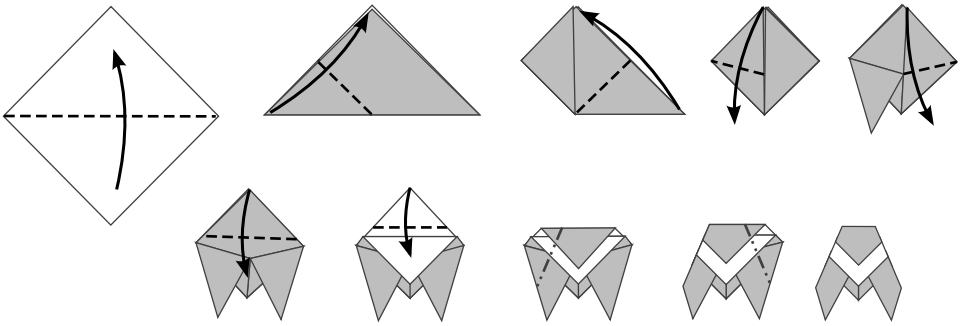

FIGURE 7. Diagrams for the traditional origami cicada model. The folding sequence was generated using our method.

the final model and the unfolded paper. The results can be used to automatically generate diagrams.

Each unfolding is checked for flat-foldability using ORIPA. From Theorem 3.7, we can conclude that all possible simple folds can be unfolded by removing one or more complete reflection paths; therefore, simply-foldability can also be checked using our method. Also, for a simply-foldable origami, all possible folding sequences using simple folds are found.

This method only focuses on flat states of the origami, not worrying about the three-dimensional intermediary states. Therefore, there is no guarantee that the simple folds can be performed without collisions, as in the rigid origami model. In other words, some folds might require some bending of the paper.

The method described here is also the basis for unfolding complex folds. We investigated the use of graph rewriting to unfold four common complex folds in order to generate folding sequences [Akitaya et al. 13].

References

[Akitaya et al. 13] Hugo A. Akitaya, Jun Mitani, Yoshihiro Kanamori, and Yukio Fukui. "Generating Folding Sequences from Crease Patterns of Flat-Foldable Origami." In *ACM SIGGRAPH 2013 Posters, SIGGRAPH '13*, pp. 20:1–20:1. New York: ACM, 2013.

[Arkin et al. 04] Esther M. Arkin, Michael A. Bender, Erik D. Demaine, Martin L. Demaine, Joseph S. B. Mitchell, Saurabh Sethia, and Steven S. Skiena. "When Can You Fold a Map?" *Computational Geometry* 29:1 (2004), 23–46. MR2080063 (2005c:52009)

[Bern and Hayes 96] Marshall Bern and Barry Hayes. "The Complexity of Flat Origami." In *Proceedings of the Seventh Annual ACM-SIAM Symposium on Discrete Algorithms*, pp. 175–183. Philadelphia: Society for Industrial and Applied Mathematics, 1996.

[Demaine and O'Rourke 07] Erik D. Demaine and Joseph O'Rourke. *Geometric Folding Algorithms: Linkages, Origami, Polyhedra*. Cambridge, UK: Cambridge University Press, 2007. MR2354878 (2008g:52001)

[Hull 94] Thomas Hull. "On the Mathematics of Flat Origamis." *Congressus Numerantium* 94 (1994), 215–224. MR1382321 (96k:05196)

[Kawasaki 91] Toshikazu Kawasaki. "On the Relation between Mountain-Creases and Valley-Creases of a Flat Origami." In *Proceedings of the First International Meeting of Origami Science and Technology*, edited by H. Huzita, pp. 229–237. Padova, Italy: Dipartimento di Fisica dell'Università di Padova, 1991.

[Lam 09] Tung Ken Lam. "Computer Origami Simulation and the Production of Origami Instructions." In *Origami^4: Fourth International Meeting of Origami Science, Mathematics, and Education*, edited by Robert J. Lang, pp. 237–250. Wellesley, MA: A K Peters, 2009. MR2590567 (2010h:00025)

[Lang 04a] Robert J. Lang. "Crease Patterns for Folders." http://www.langorigami.com/art/creasepatterns/creasepatterns_folders.php, 2004.

[Lang 04b] Robert J .Lang. “Origami Simulation." http://www.langorigami.com/science/computational/origamisim/origamisim.php, 2004.

[Lang 11] Robert J. Lang. *Origami Design Secrets: Mathematical Methods for an Ancient Art*, Second Edition. Boca Raton, FL: A K Peters/CRC Press, 2011. MR2841394

[Mitani 05] Jun Mitani. “ORIPA: Origami Pattern Editor." http://mitani.cs.tsukuba.ac.jp/oripa/, 2005.

[Robinson 04] Nick Robinson. *The Origami Bible: A Practical Guide to the Art of Paper Folding*. London: Collins & Brown, 2004.

[Smith 80] John Smith. *Pureland Origami*, Booklet 14. London: British Origami Society, 1980.

Department of Computer Science, University of Tsukuba, Japan
E-mail address: hugoakitaya@gmail.com

Department of Computer Science, University of Tsukuba, Japan
E-mail address: mitani@cs.tsukuba.ac.jp

Department of Computer Science, University of Tsukuba, Japan
E-mail address: kanamori@cs.tsukuba.ac.jp

Department of Computer Science, University of Tsukuba, Japan
E-mail address: fukui@cs.tsukuba.ac.jp

Characterization of Curved Creases and Rulings: Design and Analysis of Lens Tessellations

Erik D. Demaine, Martin L. Demaine, David A. Huffman, Duks Koschitz, and Tomohiro Tachi

1. Introduction

The past two decades have seen incredible advances in applying mathematics and computation to the analysis and design of origami made by straight creases. But, we lack many similar theorems and algorithms for origami made by curved creases.

In this chapter, we develop several basic tools (definitions and theorems) for curved-crease origami. These tools in particular characterize the relationship between the crease pattern and rule lines/segments, and they relate creases connected by rule segments. Some of these tools have been developed before in other contexts (e.g., [Fuchs and Tabachnikov 99, Fuchs and Tabachnikov 07, Huffman 76]) but have previously lacked a careful analysis of the levels of smoothness (C^1, C^2, etc.) and other assumptions required. Specific high-level properties we prove include the following:

(1) Regions between creases decompose into noncrossing rule segments, which connect from curved crease to curved crease, and planar patches (a result from [Demaine et al. 11]).
(2) The osculating plane of a crease bisects the two adjacent surface tangent planes (when they are unique).
(3) A curved crease with an incident cone ruling (a continuum of rule segments at a point) cannot fold smoothly: It must be kinked at the cone ruling.
(4) Rule segments on the convex side of a crease bend mountain/valley the same as the crease, and rule segments on the concave side of a crease bend mountain/valley opposite from the crease.
(5) If two creases are joined by a rule segment on their concave sides, or on their convex sides, then their mountain/valley assignments must be equal. If the rule segment is on the convex side of one crease and the concave side of the other crease, then the mountain/valley assignments must be opposite.

We apply these tools to analyze one family of designs called the *lens tessellation*. Figure 1 shows an example originally designed and folded by the third author in 1992, and

E. Demaine and M. Demaine supported in part by NSF ODISSEI grant EFRI-1240383 and NSF Expedition grant CCF-1138967.
D. Koschitz performed this research while at MIT.
T. Tachi supported by the JST Presto program.

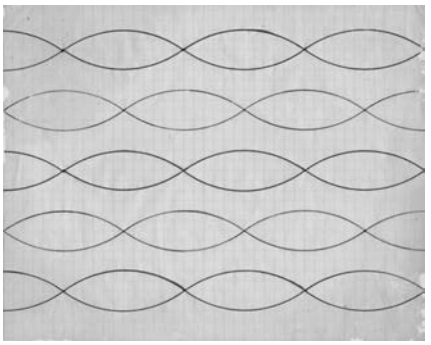

(A) Huffman's original hand-drawn sketch of crease pattern of lens design (1992).

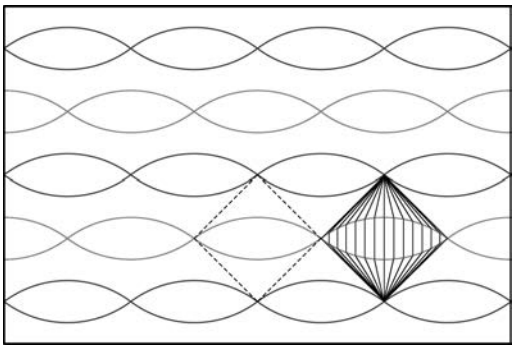

(B) Computer-drawn crease pattern of lens design.

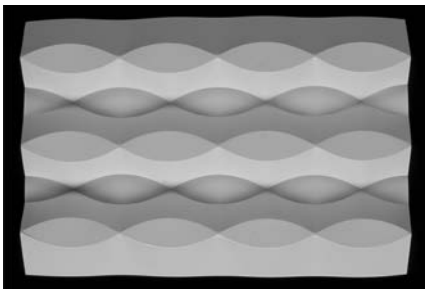

(C) Huffman's original hand-folded vinyl model (1992). Photo by Tony Grant.

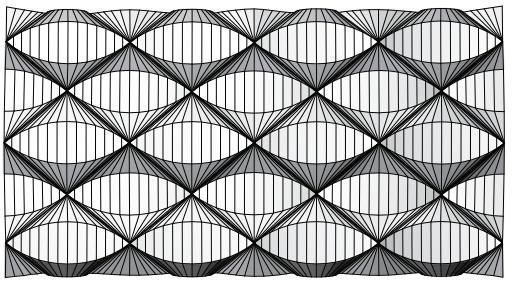

(D) Computer-simulated 3D model using Tachi's Freeform Origami software.

FIGURE 1. Lens tessellation: 1992 original (left) and digital reconstruction (right).

now modeled digitally. We prove that this curved crease pattern folds into three dimensions, with the indicated rule segments, when the "lens" is *any* smooth convex curve. We also show that the model is "rigidly foldable," meaning that it can be continuously folded without changing the ruling pattern.

The three-dimensional (3D) configuration of the curved folding is solved through identifying the correspondence between pairs of points connected by rule segments, using the qualitative properties described above. These properties separate the tessellation into independent kite-shaped tiles and force the rulings between the lenses to be particular cones with their apices coinciding with the vertices of the tiling. The ruling inside each lens is free (can twist) but, assuming no twist or global planarity/symmetry, is cylindrical (vertical rule segments). The tiling exists by rotation/reflection of the 3D model of each kite around its four straight boundary edges. From the tiling symmetry, each tile edge has a common tangent to its neighbors regardless of the type of curves, as long as it is a convex curve.

The rest of this paper is organized as follows. Section 2 introduces some basic notation for 2D and 3D curves. Section 3 defines creases, crease patterns, foldings, rule segments, cone ruling, orientation of the paper, and surface normals (and analyzes when they exist). Section 4 proves the powerful bisection property—that the osculating plane of a crease bisects the two adjacent surface tangent planes—and uses it to rule out some strange situations such as rule segments tangent to creases or zero-length rule segments. Section 5

characterizes smooth folding: A crease is folded C^1 if and only if it is folded C^2 if and only if there are no incident cone rulings. Section 6 defines mountains and valleys for both creases and the bending of rule segments, and relates the two. Finally, Section 7 uses all these tools to analyze lens tessellations, proving a necessary and sufficient condition on their foldability.

2. Curves

In this section, we define some standard parameterizations of curves in two and three dimensions, which we will use in particular for describing creases in the unfolded paper and folded state. Our notation introduces a helpful symmetry between 2D (unfolding) and 3D (folding): lowercase indicates 2D, while uppercase indicates the corresponding notion in 3D.

2.1. 2D curves. Consider an arclength-parameterized C^2 2D curve $\mathbf{x} : (0, \ell) \to \mathbb{R}^2$ (or in any metric 2-manifold). For $s \in (0, \ell)$, define the (unit) *tangent* at s by

$$\mathbf{t}(s) = \frac{d\mathbf{x}(s)}{ds}.$$

Define the *curvature*

$$k(s) = \left\| \frac{d\mathbf{t}(s)}{ds} \right\|.$$

In particular, call the curve *curved* at s if its curvature $k(s)$ is nonzero. In this case, define the (unit) *normal* at s by

$$\mathbf{n}(s) = \left. \frac{d\mathbf{t}(s)}{ds} \right/ k(s).$$

The curve is *curved* (without qualification) if it is curved at all $s \in (0, \ell)$.

Define the *convex side* at s to consist of directions having negative dot product with $\mathbf{n}(s)$, and define the *concave side* at s to consist of directions having positive dot product with $\mathbf{n}(s)$.

2.2. 3D curves. For an arclength-parameterized C^2 space curve $\mathbf{X} : [0, \ell] \to \mathbb{R}^3$, and for a parameter $s \in [0, \ell]$ inducing a point $\mathbf{X}(s)$, define the (unit) *tangent*

$$\mathbf{T}(s) = \frac{d\mathbf{X}(s)}{ds}.$$

Define the *curvature*

$$K(s) = \left\| \frac{d\mathbf{T}(s)}{ds} \right\|.$$

In particular, call the curve *curved* at s if its curvature $K(s)$ is nonzero (and *curved* without qualification if it is curved at all $s \in (0, \ell)$). In this case, define the (unit) *normal* at s by

$$\mathbf{N}(s) = \left. \frac{d\mathbf{T}(s)}{ds} \right/ K(s),$$

define the (unit) *binormal*

$$\mathbf{B}(s) = \mathbf{T}(s) \times \mathbf{N}(s),$$

and define the *torsion*

$$\tau(s) = -\frac{d\mathbf{B}(s)}{ds} \cdot \mathbf{N}(s).$$

Equivalently, these definitions follow from the Frenet–Serret formulas:

$$\begin{bmatrix} 0 & K(s) & 0 \\ -K(s) & 0 & \tau(s) \\ 0 & -\tau(s) & 0 \end{bmatrix} \cdot \begin{bmatrix} \mathbf{T}(s) \\ \mathbf{N}(s) \\ \mathbf{B}(s) \end{bmatrix} = \frac{d}{ds} \begin{bmatrix} \mathbf{T}(s) \\ \mathbf{N}(s) \\ \mathbf{B}(s) \end{bmatrix}.$$

LEMMA 2.1. *For any curved C^2 3D curve $\mathbf{X}(s)$, the Frenet frame $(\mathbf{T}(s), \mathbf{N}(s), \mathbf{B}(s))$ and curvature $K(s)$ exist and are continuous.*

PROOF. Because $\mathbf{X}(s)$ is differentiable, $\mathbf{T}(s)$ exists. Because $\mathbf{X}(s)$ is twice differentiable, $K(s)$ exists, and because $\mathbf{X}(s)$ is C^2, $K(s)$ is continuous. Because the curve is curved, $K(s) \neq 0$, so we do not divide by 0 in computing $\mathbf{N}(s)$. Thus, $\mathbf{N}(s)$ exists and is continuous. The cross product in $\mathbf{B}(s)$ exists and is continuous because $\mathbf{T}(s)$ and $\mathbf{N}(s)$ are guaranteed to be normalized (hence nonzero) and orthogonal to each other (hence not parallel). □

The same lemma specializes to 2D, by dropping the $\mathbf{B}(s)$ part:

COROLLARY 2.2. *For any curved C^2 2D curve $\mathbf{x}(s)$, the frame $(\mathbf{t}(s), \mathbf{n}(s))$ and curvature $k(s)$ exist and are continuous.*

3. Foldings

The following definitions draw from [Demaine et al. 11, Demaine and O'Rourke 07].

We start with 2D (unfolded) notions. A *piece of paper* is an open 2-manifold embedded in $\mathbb{R}^2$. A *crease* $\mathbf{x}$ is a C^2 2D curve that is contained in the piece of paper and is not self-intersecting (i.e., does not visit the same point twice). A *crease point* is a point $\mathbf{x}(s)$ on the relative interior of the crease (excluding endpoints). The endpoints of a crease are *vertices*. A *crease pattern* is a collection of creases that meet only at common vertices. Equivalently, a crease pattern is an embedded planar graph, where each edge is embedded as a crease. This definition effectively allows piecewise-C^2 curves, by subdividing the edge in the graph with additional vertices; "creases" are the resulting C^2 pieces. A *face* is a maximal open region of the piece of paper not intersecting any creases or vertices.

Now we proceed to 3D (folded) notions. A *(proper) folding* of a crease pattern is a piecewise-C^2 isometric embedding of the piece of paper into three dimensions that is C^1 on every face and not C^1 at every crease point and vertex. Here, *isometric* means that intrinsic path lengths are preserved by the mapping, and *piecewise-C^2* means that the folded image can be decomposed into a finite complex of C^2 open regions joined by points and C^2 curves. We use the terms *folded crease*, *folded vertex*, *folded face*, and *folded piece of paper* to refer to the image of a crease, vertex, face, and entire piece of paper under the folding map, respectively. Thus, each folded face subdivides into a finite complex of C^2 open regions joined by points called *folded semivertices* and C^2 curves called *folded semicreases*. Each folded crease $\mathbf{X}(s)$ can be subdivided into a finite sequence of C^2 curves joined by C^1 points called *semikinks* and not-C^1 points called *kinks*. (Here, C^1/not-C^1 is a property measured of the crease $\mathbf{X}(s)$; crease points are necessarily not C^1 on the folded piece of paper.) In fact, semivertices do not exist [Demaine et al. 11, Corollary 2] and neither do semikinks (Corollary 6.4 below).

LEMMA 3.1. *A curved crease $\mathbf{x}(s)$ folds into a 3D curve $\mathbf{X}(s)$ that contains no line segments (and thus is curved except at kinks and semikinks).*

PROOF. Suppose $X(s)$ is a 3D line segment for $s \in [s_1, s_2]$. Then, the distance between $\mathbf{X}(s_1)$ and $\mathbf{X}(s_2)$ as measured on the folded piece of paper is the length of this line segment, i.e., the arclength of $\mathbf{X}$ over $s \in [s_1, s_2]$, which, by isometry, equals the arclength of $\mathbf{x}$ over

$s \in [s_1, s_2]$. However, in the 2D piece of paper, there is a shorter path connecting $\mathbf{x}(s_1)$ and $\mathbf{x}(s_2)$ because the 2D crease is curved (and not on the paper boundary, because the paper is an open set), contradicting isometry. □

3.1. Developable surfaces. A folded face is also known as an uncreased developable surface: it is *uncreased* in the sense that it is C^1, and it is *developable* in the sense that every point p has a neighborhood isometric to a region in the plane. The following theorem from [Demaine et al. 11] characterizes what uncreased developable surfaces look like:

THEOREM 3.2 (Corollaries 1–3 of [Demaine et al. 11]). *Every interior point p of an uncreased developable surface M not belonging to a planar neighborhood belongs to a unique rule segment C_p. The rule segment's endpoints are on the boundary of M. In particular, every semicrease is such a rule segment.*

COROLLARY 3.3. *Any folded face decomposes into planar regions and nonintersecting rule segments (including semicreases) whose endpoints lie on creases.*

For a folded piece of paper, we use the term *(3D) rule segment* for exactly these segments C_p computed for each folded face, for all points p that are not folded vertices, are not folded crease points, and do not belong to a planar neighborhood. In particular, we view the interior of planar regions as not containing any rule segments (as they would be ambiguous); however, the boundaries of planar regions are considered rule segments. As a consequence, all rule segments have a neighborhood that is nonplanar.

For each 3D rule segment in the folded piece of paper, we can define the corresponding 2D rule segment by the inverse mapping. By isometry, 2D rule segments are indeed line segments.

Define a *cone ruling* at a crease point $\mathbf{x}(s)$ to be a fan of 2D rule segments emanating from $\mathbf{x}(s)$ in a positive-length interval of directions $[\theta_1, \theta_2]$.

3.2. Orientation. We orient the piece of paper in the xy-plane by a consistent normal $\mathbf{e}_z$ (in the $+z$ direction) called the *top side*. This orientation defines, for a 2D crease $\mathbf{x} = \mathbf{x}(s)$ in the crease pattern, a *left normal* $\hat{\mathbf{n}}(s) = \mathbf{e}_z \times \mathbf{t}(s)$. Where $\mathbf{x}(s)$ is curved and thus $\mathbf{n}(s)$ is defined, we have $\hat{\mathbf{n}}(s) = \pm\mathbf{n}(s)$ where the sign specifies whether the left or right side corresponds to the convex side of the curve. We can also characterize a 2D rule segment incident to $\mathbf{x}(s)$ as being *left* of $\mathbf{x}$ when the vector emanating from $\mathbf{x}(s)$ has positive dot product with $\hat{\mathbf{n}}(s)$ and *right* of $\mathbf{x}$ when it has negative dot product. (In Lemma 4.6 below, we prove that no rule segment is tangent to a crease, and thus every rule segment is either left or right of the crease.)

We can also define the *signed curvature* $\hat{k}(s)$ to flip sign where $\hat{\mathbf{n}}(s)$ does: $\hat{k}(s)\hat{\mathbf{n}}(s) = k(s)\mathbf{n}(s)$. Then, $\hat{k}(s)$ is positive where the curve turns left and negative where the curve turns right (relative to the top side).

3.3. Unique ruling. Call a crease point $\mathbf{x}(s)$ *uniquely ruled on the left* if there is exactly one rule segment left of $\mathbf{x}(s)$; symmetrically define *uniquely ruled on the right*; and define *uniquely ruled* to mean uniquely ruled on both the left and right.

By Corollary 3.3, there are two possible causes for a crease point $\mathbf{x}(s)$ to be not uniquely ruled (say, on the left). First, there could be one or more cone rulings (on the left) at $\mathbf{x}(s)$. Second, there could be one or more planar 3D regions incident to $\mathbf{X}(s)$ (which, in 2D, lie on the left of $\mathbf{x}(s)$, meaning the points have positive dot product with $\hat{\mathbf{n}}(s)$).

One special case of unique ruling is when a rule segment is tangent to a curved crease. Ultimately, in Lemma 4.6, we will prove that this cannot happen, but for now we need that the surface normals remain well-defined in this case. There are two subcases depending on

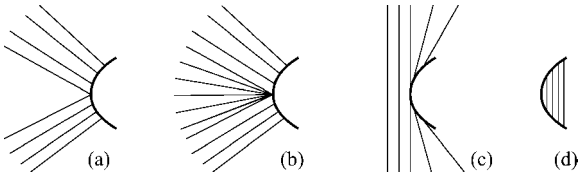

FIGURE 2. Possibilities for a crease to be not uniquely ruled.

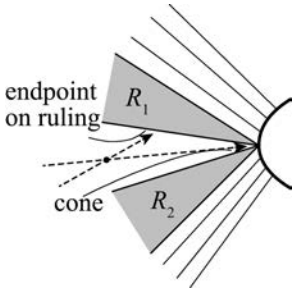

FIGURE 3. Two adjacent planar regions at a point.

whether the rule segment is on the convex or concave side of the crease, as in Figure 2(c) and (d). The rule segment's direction in 3D and surface normal vector remain well-defined in this case, by taking limits of nearby rule segments. In the concave subcase (d), we take the limit of rule segments on the same side of the curve. In the convex subcase (c), the rule segment splits the surface locally into two halves, and we take the limit of rule segments in the half not containing the crease. Because the surface normals are thus well-defined, we do not need to distinguish this case in our proofs below.

Call a crease point $\mathbf{x}(s)$ *cone free* if there are no cone rulings at $\mathbf{x}(s)$; similarly define *cone free on the left/right*. Such a point may still have a planar region, but only one.

LEMMA 3.4. *If a crease point* $\mathbf{x}(s)$ *is cone free, then it has at most one planar region on each side.*

PROOF. Refer to Figure 3. Suppose $\mathbf{x}(s)$ had at least two planar regions on, say, the left side. Order the regions clockwise around $\mathbf{x}(s)$, and pick two adjacent planar regions R_1 and R_2. By Corollary 3.3, the wedge with apex $\mathbf{x}(s)$ between R_1 and R_2 must be covered by rule segments. But, by Theorem 3.2, a rule segment cannot have its endpoints on the boundaries of R_1 and R_2, as it must extend all the way to creases. Thus, the only way to cover the wedge locally near $\mathbf{x}(s)$ is to have a cone ruling at $\mathbf{x}(s)$. □

3.4. Surface normals. In 3D, the orientation defines a top-side normal vector at every C^1 point.[1] For a crease point $\mathbf{X}(s)$ that is cone free on the left, we can define a unique *left surface normal* $\mathbf{P}_L(s)$. First, if there is a planar region on the left of $\mathbf{X}(s)$, then by Lemma 3.4 there is only one such planar region, and we define $\mathbf{P}_L(s)$ to be the unique top-side normal vector of the planar region. Otherwise, $\mathbf{X}(s)$ is uniquely ruled on the left, and we define $P_L(s)$ to be the top-side surface normal vector that is constant along this unique rule segment. (As argued above, this definition makes sense even when the rule segment

[1]For example, take infinitesimally small triangles around the point, oriented counterclockwise in 2D, and compute their normals in 3D.

is a zero-length limit of rule segments.) Similarly, we can define the right surface normal $\mathbf{P}_R(s)$ when $\mathbf{X}(s)$ is cone free on the right.

4. Bisection Property

In this section, we prove that, at a cone-free folded curved crease, the binormal vector bisects the left and right surface normal vectors, which implies that the osculating plane of the crease bisects the two surface tangent planes. Proving this bisection property requires several steps along the way, and it has several useful consequences.

4.1. C^2 case. First, we prove the bisection property at C^2 crease points, using the following simple lemma:

LEMMA 4.1. *For a C^2 folded curved crease $\mathbf{X}(s)$ that is cone-free on the left,*

$$(K(s)\mathbf{N}(s)) \cdot (\mathbf{P}_L(s) \times \mathbf{T}(s)) = \hat{\mathbf{k}}(s).$$

For a C^2 folded curved crease $\mathbf{X}(s)$ that is cone-free on the right,

$$(K(s)\mathbf{N}(s)) \cdot (\mathbf{P}_R(s) \times \mathbf{T}(s)) = \hat{\mathbf{k}}(s).$$

PROOF. We prove the left case; the right case is symmetric. The left-hand side is known as the geodesic curvature at $\mathbf{X}(s)$ on surface S_L and is known to be invariant under isometry. In the unfolded 2D state, the geodesic curvature is

$$(k(s)\mathbf{n}(s)) \cdot (\mathbf{e}_z \times \mathbf{t}(s)) = (k(s)\mathbf{n}(s)) \cdot \hat{\mathbf{n}}(s) = \hat{k}(s).$$

□

LEMMA 4.2. *For a C^2 cone-free folded curved crease $\mathbf{X}(s)$, $\mathbf{B}(s)$ bisects $\mathbf{P}_L(s)$ and $\mathbf{P}_R(s)$. In particular, the tangent planes of the surfaces on both sides of $\mathbf{X}(s)$ form the same angle with the osculating plane.*

PROOF. A C^2 cone-free folded curved crease $\mathbf{X}(s)$ has unique left and right surface normals $\mathbf{P}_L(s)$ and $\mathbf{P}_R(s)$. By Lemma 4.1, the left and right geodesic curvatures match:

$$(K(s)\mathbf{N}(s)) \cdot (\mathbf{P}_L(s) \times \mathbf{T}(s)) = (K(s)\mathbf{N}(s)) \cdot (\mathbf{P}_R(s) \times \mathbf{T}(s)).$$

The $K(s)$ scalars cancel, leaving a triple product:

$$\mathbf{N}(s) \cdot (\mathbf{P}_L(s) \times \mathbf{T}(s)) = \mathbf{N}(s) \cdot (\mathbf{P}_R(s) \times \mathbf{T}(s)),$$

which is equivalent to

$$\mathbf{P}_L(s) \cdot (\mathbf{T}(s) \times \mathbf{N}(s)) = \mathbf{P}_R(s) \cdot (\mathbf{T}(s) \times \mathbf{N}(s)).$$

Therefore, $\mathbf{B}(s) = \mathbf{T}(s) \times \mathbf{N}(s)$ forms the same angle with $\mathbf{P}_L(s)$ and $\mathbf{P}_R$. Because $\mathbf{B}$, $\mathbf{P}_L$, and $\mathbf{P}_R$ lie in a common plane orthogonal to $\mathbf{T}$, $\mathbf{B}$ bisects $\mathbf{P}_L$ and $\mathbf{P}_R$. □

4.2. Top-side Frenet frame. By Lemma 4.2, at C^2 cone-free points $\mathbf{X}(s)$, we can define the *top-side normal* of the osculating plane $\hat{\mathbf{B}} = \pm\mathbf{B} = \pm\mathbf{T}\times\mathbf{N}$ whose sign is defined such that $\hat{\mathbf{B}}\cdot\mathbf{P}_L = \hat{\mathbf{B}}\cdot\mathbf{P}_R > 0$. Thus, $\hat{\mathbf{B}}$ consistently points to the front side of the surface. By contrast, $\mathbf{B}$'s orientation depends on whether the 2D curve locally turns left or right (given by the sign of $k(s)$), flipping orientation at inflection points (where $k(s) = 0$).

More formally, we will use the *top-side Frenet frame* given by $(\mathbf{T}(s), \hat{\mathbf{N}}(s), \hat{\mathbf{B}}(s))$, where $\hat{\mathbf{N}}(s) = \hat{\mathbf{B}}(s) \times \mathbf{T}(s)$.

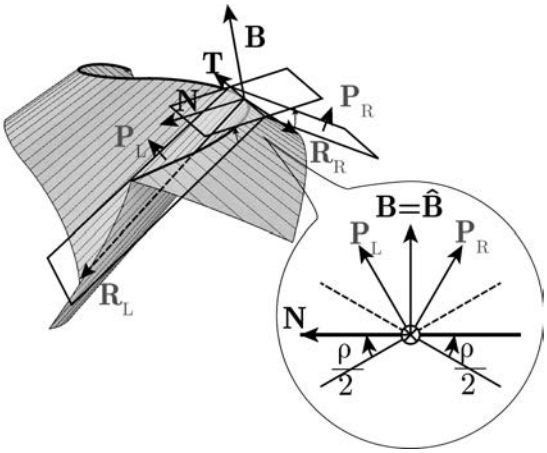

FIGURE 4. Binormal vector $\mathbf{B}$ bisects surface normals $\mathbf{P}_L$ and $\mathbf{P}_R$.

LEMMA 4.3. *Consider a folded curved crease* $\mathbf{X}(s)$ *that is cone-free at a semikink* $s = \tilde{s}$. *The top-side Frenet frames are identical in positive and negative limits:*

$$\lim_{s\to\tilde{s}^+}(\mathbf{T}(s), \hat{\mathbf{N}}(s), \hat{\mathbf{B}}(s)) = \lim_{s\to\tilde{s}^-}(\mathbf{T}(s), \hat{\mathbf{N}}(s), \hat{\mathbf{B}}(s)).$$

Thus, the top-side Frenet frame is continuous at $s = \tilde{s}$.

PROOF. First, $\mathbf{T}(\tilde{s})$ is continuous because $\mathbf{X}(s)$ is C^1 at a semikink $s = \tilde{s}$.

Second, by Lemma 4.2, in the positive and negative limits, $\mathbf{B}(s)$ bisects $\mathbf{P}_L(s)$ and $\mathbf{P}_R(s)$. Because there is no cone ruling at $s = \tilde{s}$, the left and right surface normals $\mathbf{P}_L(s)$ and $\mathbf{P}_R(s)$ have equal positive and negative limits at $\tilde{s}$, so $\mathbf{P}_L(\tilde{s})$ and $\mathbf{P}_R(\tilde{s})$ are continuous. Thus, $\mathbf{B}(\tilde{s}^+)$ and $\mathbf{B}(\tilde{s}^-)$ must lie on a common bisecting line of $\mathbf{P}_L(\tilde{s})$ and $\mathbf{P}_R(\tilde{s})$, and $\hat{\mathbf{B}}(\tilde{s})$ is uniquely defined by having positive dot product with $\mathbf{P}_1(\tilde{s})$ and $\mathbf{P}_2(\tilde{s})$. This gives us a unique definition of $\hat{\mathbf{B}}(s)$.

Third, $\hat{\mathbf{N}}(s)$ is continuous as $\hat{\mathbf{B}}(s) \times \mathbf{T}(s)$. Therefore, $(\mathbf{T}(s), \hat{\mathbf{N}}(s), \hat{\mathbf{B}}(s))$ is continuous at $s = \tilde{s}$. □

At C^2 points $X(s)$, we can define the *signed curvature* $\hat{K}(s)$ to flip sign where $\hat{\mathbf{N}}(s)$ does: $\hat{K}(s)\hat{\mathbf{N}}(s) = K(s)\mathbf{N}(s)$. As in 2D, $\hat{K}(s)$ is positive where the curve turns left and negative where the curve turns right (relative to the top side).

4.3. General bisection property. By combining Lemmas 4.2 and 4.3, we obtain a stronger bisection lemma:

COROLLARY 4.4. *For a cone-free folded curved crease* $\mathbf{X}(s)$, $\hat{\mathbf{B}}(s)$ *bisects* $\mathbf{P}_L(s)$ *and* $\mathbf{P}_R(s)$. *In particular, the tangent planes of the surfaces on both sides of* $\mathbf{X}(s)$ *form the same angle with the osculating plane.*

4.4. Consequences. Using the bisector property, we can prove the nonexistence of a few strange situations.

LEMMA 4.5. *A crease* $\mathbf{X}$ *curved at* s *cannot have a positive-length interval* $s \in (s - \varepsilon, s + \varepsilon)$ *incident to a planar region.*

PROOF. If this situation were to happen, then the osculating plane of the curve must equal the plane of the planar region, which is, say, the left surface plane. By Corollary 4.4,

the right surface plane must be the same plane. But then, the folded piece of paper is actually planar along the crease, contradicting that it is not C^1 along the crease. □

LEMMA 4.6. *A rule segment cannot be tangent to a cone-free curved crease point (at a relative interior point, in 2D or 3D).*

PROOF. Suppose by symmetry that a rule segment is tangent to a crease point on its left side. If a rule segment is tangent to the crease point $\mathbf{x}(s)$ in 2D, then it must also be tangent to $\mathbf{X}(s)$ in 3D. There are two cases: (1) The left surface is a tangent surface generated from the crease, and (2) the surface is trimmed by the crease and is only tangent at the point $\mathbf{X}(s)$.

In Case 1, there is a finite portion of the crease that is C^2 and tangent to the incident rule segment. Then, for that portion of the crease (including s), the tangent plane of the left surface is the osculating plane of the curve.

In Case 2, consider surface normal $\mathbf{P}_L(s)$ at $\mathbf{X}(s)$. By assumption, the tangent vector $\mathbf{T}$ is parallel to the rule segment incident to $\mathbf{X}(s)$. Suppose by symmetry that $\mathbf{T}$ is actually the direction of the rule segment from $\mathbf{X}(s)$. (Otherwise, we could invert the parameterization of $\mathbf{X}$.) Because the surface normal is constant along the rule segment, and thus in the rule-segment direction, we have

$$\frac{d\mathbf{P}_L}{ds^+} = \mathbf{0}.$$

Because $\mathbf{P}_L$ and $\mathbf{T}$ are perpendicular, $\frac{d}{ds^+}(\mathbf{P}_L \cdot \mathbf{T}) = 0$, which expands to

$$\frac{d\mathbf{P}_L}{ds^+} \cdot \mathbf{T} + \mathbf{P}_L \cdot \frac{d\mathbf{T}}{ds^+} = 0.$$

Thus, we obtain $\mathbf{P}_L \cdot \frac{d\mathbf{T}}{ds^+} = 0$. Because the folded crease is not straight (Lemma 3.1), $\mathbf{N}$ is perpendicular to $\mathbf{P}_L$. Therefore, the left tangent plane equals the osculating plane.

By Corollary 4.4, in either case, the right tangent plane must also equal the osculating plane, meaning that the folded piece of paper is actually planar along the crease, contradicting that it is not C^1 along the crease. □

When the crease is C^2, Lemma 4.6 also implicitly follows from the Fuchs–Tabachnikov relation between fold angle and rule-segment angle [Fuchs and Tabachnikov 99], [Fuchs and Tabachnikov 07].

COROLLARY 4.7. *For a crease* $\mathbf{X}$ *curved and cone-free at* s*, the point* $\mathbf{X}(s)$ *has an incident positive-length rule segment on the left side of* $\mathbf{X}$ *and an incident positive-length rule segment on the right side of* $\mathbf{X}$.

PROOF. First, by Lemma 4.5, $\mathbf{X}(s)$ is not locally surrounded by a flat region on either side, so by Corollary 3.3, $\mathbf{X}(s)$ must have a rule segment on its left and right sides. Furthermore, such a rule segment cannot be a zero-length limit of nearby rule segments, because such a rule segment would be tangent to the curve, contradicting Lemma 4.6. □

COROLLARY 4.8. *If a face's boundary is a* C^1 *curved closed curve, then the folded face's boundary is not* C^1.

PROOF. Consider the decomposition from Corollary 3.3 applied to the face, resulting in planar and ruled regions. By Lemma 4.5, the ruled regions' boundaries collectively cover the face boundary. The planar regions form a laminar (noncrossing) family in the face, so there must be a ruled region adjacent to only one planar region (or zero if the entire folded face is ruled). This ruled region is either the entire folded face or bounded by a portion of

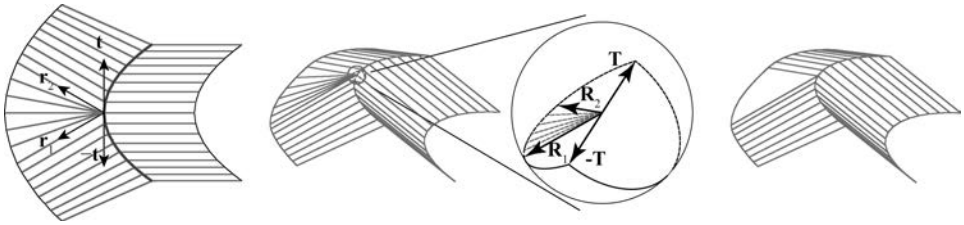

FIGURE 5. Cone rulings must fold into a kink in 3D.

the face boundary and by a single rule segment (bounding a planar region). For each rule segment in the ruled region, we can discard the side that (possibly) contains the boundary rule segment, effectively shrinking the rule region while preserving its boundary structure of partial face boundary and one rule segment. In the limit of this process, we obtain a rule segment that is tangent to the face boundary. By Lemma 4.6, this situation can happen only if the face is cone ruled at some point, which by Theorem 5.1 implies that the folded face boundary is not C^1. □

5. Smooth Folding

A *smoothly folded crease* is a folded crease that is C^1, i.e., kink-free. In Corollary 6.4 below, we will show that a smoothly folded crease is furthermore C^2, i.e., it cannot have semikinks. A *smooth folding* of a crease pattern is a folding in which every crease is smoothly folded. In this section, we characterize smooth folding as cone-free.

THEOREM 5.1. *If a folded crease* $\mathbf{X}$ *has a cone ruling at a point* $\mathbf{X}(s)$*, then* $\mathbf{X}$ *is kinked at* s*.*

PROOF. Assume by symmetry that $\mathbf{X}(s)$ has a cone ruling on the left side, say clockwise from rule vector $\mathbf{R}_1$ to rule vector $\mathbf{R}_2$. Because the unfolded crease $\mathbf{x}$ is C^1, it has a tangent vector $\mathbf{t}$, so the left side of $\mathbf{x}(s)$ is, to the first order, the cone clockwise from $-\mathbf{t}$ to $\mathbf{t}$. Thus, we have $-\mathbf{t}$, $\mathbf{r}_1$, $\mathbf{r}_2$, and $\mathbf{t}$ appearing in clockwise order around $\mathbf{x}(s)$, giving us the angle following relation:

$$180^\circ = \angle(-\mathbf{t}, \mathbf{t}) = \angle(-\mathbf{t}, \mathbf{r}_1) + \angle(\mathbf{r}_1, \mathbf{r}_2) + \angle(\mathbf{r}_2, \mathbf{t}).$$

Now assume for contradiction that $\mathbf{X}$ is C^1 at s, so we can define the tangent vector $\mathbf{T}(s)$. By triangle inequality on the sphere, we have

$$180^\circ = \angle(-\mathbf{T}, \mathbf{T}) \leq \angle(-\mathbf{T}, \mathbf{R}_1) + \angle(\mathbf{R}_1, \mathbf{R}_2) + \angle(\mathbf{R}_2, \mathbf{T}).$$

The latter three 3D angles must be smaller than or equal to the corresponding angles in 2D, by isometry. Furthermore, $\angle(R_1, R_2) < \angle(\mathbf{r}_1, \mathbf{r}_2)$, because the surface must be bent along the entire cone ruling (otherwise it would have a flat patch). Therefore,

$$\angle(-\mathbf{T}, \mathbf{R}_1) + \angle(\mathbf{R}_1, \mathbf{R}_2) + \angle(\mathbf{R}_2, \mathbf{T}) < \angle(-\mathbf{t}, \mathbf{r}_1) + \angle(\mathbf{r}_1, \mathbf{r}_2) + \angle(\mathbf{r}_2, \mathbf{t}) = 180^\circ,$$

a contradiction. □

Now we get a characterization of smooth folding:

COROLLARY 5.2. *A folded curved crease* $\mathbf{X}$ *is kinked at* s *if and only if it has a cone ruling at* $\mathbf{X}(s)$*.*

Proof. Theorem 5.1 proves the "if" implication.

To prove the converse, consider a cone-free crease point $\mathbf{X}(s)$. In 2D, we have a $180^\circ = \angle(-\mathbf{t}, \mathbf{t})$ angle on either side of the crease. We claim that this 180° angle between the backward tangent and forward tangent is preserved by the folding, so the folded crease $\mathbf{X}$ has a continuous tangent and thus is C^1 at s.

First, suppose that there is no planar region incident to $\mathbf{X}(s)$ on, say, the left side. Then, the left side is locally a uniquely ruled C^2 surface, with no rule segments tangent to the curve by Lemma 4.6, and thus the surface can be extended slightly to include $\mathbf{X}(s)$ in its interior. In a C^1 surface, it is known that geodesic (2D) angles equal Euclidean (3D) angles, so folding preserves the 180° angle between the backward and forward tangents.

Now suppose that there is a planar region on the left side of $\mathbf{X}(s)$. By Lemma 3.4, there can be only one, and by Lemma 4.5, there must be two uniquely ruled surfaces separating such a planar region from the crease. These three surfaces meet smoothly with a common surface normal, as the surface is C^2 away from the crease, so the overall angle between the backward and forward tangents of the crease equals the sum of the three angles of the surfaces at $\mathbf{X}(s)$. The previous paragraph argues that the two uniquely ruled surfaces preserve their angles, and the planar region clearly preserves its angle (it is not folded). Hence, again, folding preserves the 180° angle between the backward and forward tangents. □

6. Mountains and Valleys

6.1. Crease. Refer to Figure 4. For a smoothly folded (cone-free) crease $\mathbf{X}$, the *fold angle* $\rho \in (-180^\circ, 180^\circ)$ at $\mathbf{X}(s)$ is defined by $\cos\rho = \mathbf{P}_L \cdot \mathbf{P}_R$ and $\sin\rho = [(\mathbf{P}_L \times \mathbf{P}_R) \cdot \mathbf{T}]$. The crease is *valley* at s if the fold angle is negative, i.e., $(\mathbf{P}_L \times \mathbf{P}_R) \cdot \mathbf{T} < 0$. The crease is *mountain* at s if the fold angle is positive, i.e., $(\mathbf{P}_L \times \mathbf{P}_R) \cdot \mathbf{T} > 0$.

Lemma 6.1. *A smoothly folded curved crease* $\mathbf{X}$ *has a continuous fold angle* $\rho \neq 0$.

Proof. By Corollary 5.2, the crease is cone-free, so the surface normals $\mathbf{P}_L(s)$ and $\mathbf{P}_R(s)$ are continuous. If the resulting fold angle $\rho(s)$ were zero, then we would have $\mathbf{P}_L(s) = \mathbf{P}_R(s)$, contradicting that the folded piece of paper is not C^1 at crease point $\mathbf{X}(s)$. □

Corollary 6.2. *A smoothly folded curved crease* $\mathbf{X}$ *is mountain or valley throughout.*

Proof. By Lemma 6.1, $\rho(s)$ is continuous and nonzero. By the intermediate value theorem, $\rho(s)$ cannot change sign. □

Lemma 6.3. *For a smoothly folded curved crease* $\mathbf{X}(s)$*,*

$$\hat{K}(s) \cos\frac{1}{2}\rho(s) = \hat{k}(s).$$

In particular, folding increases curvature: $|\hat{k}(s)| < |\hat{K}(s)|$*, i.e.,* $k(s) < K(s)$*.*

Proof. Referring to Figure 4, we have

$$\cos\frac{1}{2}\rho(s) = \mathbf{P}_L(s) \cdot \hat{\mathbf{B}}(s).$$

By definition of $\hat{\mathbf{B}}(s)$, this dot product is the triple product

$$\mathbf{P}_L(s) \cdot (\mathbf{T}(s) \times \hat{\mathbf{N}}(s)) = \hat{\mathbf{N}}(s) \cdot (\mathbf{P}_L(s) \times \mathbf{T}(s))$$

(similar to the proof of Lemma 4.2). Multiplying by $\hat{K}(s)$, we obtain

$$(\hat{K}(s)\hat{\mathbf{N}}(s)) \cdot (\mathbf{P}_L(s) \times \mathbf{T}(s)) = (K(s)N(s)) \cdot (\mathbf{P}_L(s) \times \mathbf{T}(s)).$$

By Lemma 4.1, this geodesic curvature is $\hat{\mathbf{k}}(s)$. □

Corollary 6.4. *A folded crease cannot have a semikink, and thus a smoothly folded crease* $\mathbf{X}$ *is* C^2.

Proof. Suppose $\mathbf{X}(s)$ had a semikink at $s = \tilde{s}$. Applying Lemma 6.3 with positive and negative limits, we obtain that

$$\lim_{s \to \tilde{s}^+} \hat{K}(s) = \frac{\hat{k}(s)}{\cos \frac{1}{2}\rho} = \lim_{s \to \tilde{s}^-} \hat{K}(s),$$

and thus the signed curvature $\hat{K}(s)$ is continuous at $s = \tilde{s}$. By Lemma 4.3, $\hat{\mathbf{N}}(s)$ is continuous at $s = \tilde{s}$. Therefore, $\frac{d^2\mathbf{X}(s)}{ds^2} = \hat{K}(s)\hat{\mathbf{N}}(s)$ is continuous at $s = \tilde{s}$, so $\mathbf{X}(\tilde{s})$ is not actually a semikink. □

Lemma 6.5. *A smoothly folded crease* $\mathbf{X}$ *is valley if and only if* $(\mathbf{P}_L \times \hat{\mathbf{B}}) \cdot \mathbf{T} < 0$*, and mountain if and only if* $(\mathbf{P}_L \times \hat{\mathbf{B}}) \cdot \mathbf{T} > 0$.

Proof. Refer to Figure 4. Vectors $\mathbf{P}_L$, $\mathbf{P}_R$, and $\hat{\mathbf{B}}$ are all perpendicular to $\mathbf{T}$ and thus live in a common oriented plane with normal $\mathbf{T}$. By the choice of $\hat{\mathbf{B}}$ to have positive dot products with $\mathbf{P}_L$ and $\mathbf{P}_R$, the three vectors in fact live in a common half-plane. In this plane, we can see the fold angle $\rho = \angle(\mathbf{P}_L, \mathbf{P}_R)$, where $\angle$ measures the convex angle between the vectors, signed positive when the angle is convex in the counterclockwise orientation within the oriented plane with normal $\mathbf{T}$ and signed negative when clockwise.

By Corollary 4.4, $\mathbf{P}_L \cdot \mathbf{B} = \mathbf{P}_R \cdot \mathbf{B}$, so $\mathbf{P}_L \cdot \hat{\mathbf{B}} = \mathbf{P}_R \cdot \hat{\mathbf{B}}$. Thus, $\cos \angle(\mathbf{P}_L, \hat{\mathbf{B}}) = \cos \angle(\mathbf{P}_R, \hat{\mathbf{B}})$, i.e., $|\angle(\mathbf{P}_L, \hat{\mathbf{B}})| = |\angle(\mathbf{P}_R, \hat{\mathbf{B}})|$.

If $\angle(\mathbf{P}_L, \hat{\mathbf{B}}) = \angle(\mathbf{P}_R, \hat{\mathbf{B}})$, then $\mathbf{P}_L = \mathbf{P}_R$, contradicting that $\mathbf{X}$ is a crease. Therefore, $\angle(\mathbf{P}_L, \hat{\mathbf{B}}) = \angle(\hat{\mathbf{B}}, \mathbf{P}_R) = \pm\frac{1}{2}\angle(\mathbf{P}_L, \mathbf{P}_R)$. Because $|\angle(\mathbf{P}_L, \hat{\mathbf{B}})| < 90°$, we must in fact have $\angle(\mathbf{P}_L, \hat{\mathbf{B}}) = \angle(\hat{\mathbf{B}}, \mathbf{P}_R) = \frac{1}{2}\angle(\mathbf{P}_L, \mathbf{P}_R)$, i.e., $\hat{\mathbf{B}}$ bisects the convex angle $\angle(\mathbf{P}_L, \mathbf{P}_R)$. Hence, $\hat{\mathbf{B}}$ lies in between $\mathbf{P}_L$ and $\mathbf{P}_R$ within the half-plane. Therefore, the cross products $\mathbf{P}_L \times \mathbf{P}_R$, $\mathbf{P}_L \times \hat{\mathbf{B}}$, and $\hat{\mathbf{B}} \times \mathbf{P}_R$ are all parallel, so their dot products with $\mathbf{T}$ have the same sign. □

6.2. Rule segment. We can also define whether a rule segment bends the paper mountain or valley; refer to Figure 6. Consider a relative interior point $\mathbf{Y}$ of a rule segment with direction vector $\mathbf{R}$, with top-side surface normal $\mathbf{P}$. Then, we can construct a local Frenet frame at $\mathbf{Y}$ with tangent vector $\mathbf{Q} = \mathbf{R} \times \mathbf{P}$, normal vector $\mathbf{P}$, and binormal vector $\mathbf{R}$. These frames define a 3D curve $\mathbf{Y}(t)$, where $\mathbf{Y}(0) = \mathbf{Y}$, which follows the principle curvature of the surface. Parameterize this curve by arclength.

First, consider the case when the surface is C^2 at $Y(t)$. The surface *bends valley* at $\mathbf{Y}(t)$ if the curvature vector $\frac{d^2\mathbf{Y}(t)}{dt^2} = \frac{d\mathbf{Q}(t)}{dt}$ is on the top side, i.e., has positive dot product with $\mathbf{P}(t)$; and it *bends mountain* if $\frac{d\mathbf{Q}(t)}{dt} \cdot \mathbf{P}(t) < 0$. In particular, at $t = 0$, we determine whether the original rule segment bends mountain or valley at $\mathbf{Y}$.

If the surface is not C^2 at $Y(t)$, then the rule segment is a semicrease, which connects two C^2 surfaces sharing a surface normal at the crease; refer to Figure 7. In this case, the surface bends valley at $\mathbf{Y}(t)$ when the two surfaces bend valley or when one of the surfaces is planar and the other bends valley. Similarly, the surface bends mountain at $\mathbf{Y}(t)$ when the two surfaces bend mountain or one of the surfaces is planar and the other bends mountain. At an inflection point, there is no mountain/valley assignment.

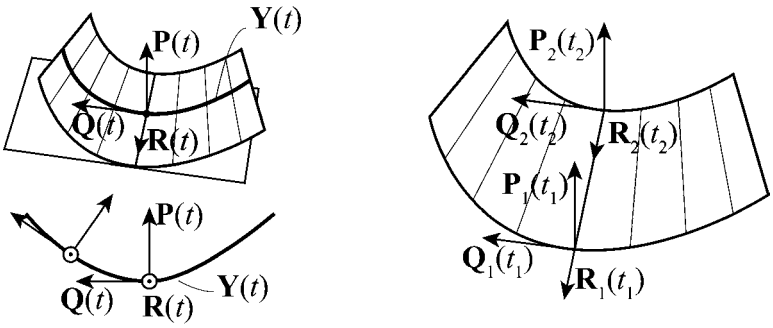

FIGURE 6. Defining a frame around an interior point to define mountain versus valley bending.

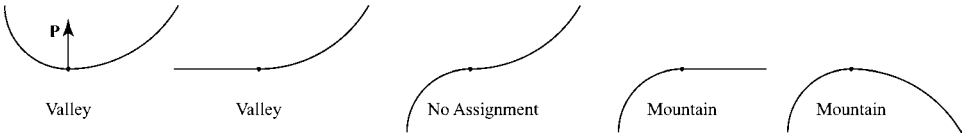

FIGURE 7. Definition of mountain and valley for a semicrease.

LEMMA 6.6. *A developable uncreased surface bends the same direction (mountain or valley) at every relative interior point of a rule segment.*

PROOF. First, consider the case when the surface is C^2. Consider two points $\mathbf{Y}_1$ and $\mathbf{Y}_2$ on the rule segment, with principle curvature frames $(\mathbf{Q}_i(t_i), \mathbf{R}_i(t_i), \mathbf{P}_i(t_i))$. Choose t_2 as a function of t_1 such that $\mathbf{Y}_1(t_1)$ and $\mathbf{Y}_2(t_2)$ lie on a common rule segment. Then, the frames are in fact identical: $\mathbf{R}_1(t_1) = \mathbf{R}_2(t_2)$ is the common rule direction, $\mathbf{P}_1(t_1) = \mathbf{P}_2(t_2)$ is the common top-side surface normal, and $\mathbf{Q}_1(t_1) = \mathbf{Q}_2(t_2)$ is their cross product. Because the surface is locally C^2 around the ruled segment $\mathbf{Y}_1$ and $\mathbf{Y}_2$, we have $\frac{dt_2}{dt_1} > 0$, so

$$\frac{d\mathbf{Q}_2(t_2)}{dt_2} \cdot \mathbf{P} = \frac{d\mathbf{Q}_1(t_1)}{dt_2} \cdot \mathbf{P} = \frac{dt_2}{dt_1} \frac{d\mathbf{Q}_1(t_1)}{dt_1} \cdot \mathbf{P}.$$

Therefore, the surface bends the same direction.

Next, consider the case when the surface is not C^2, i.e., the rule segment is a semicrease between C^2 surfaces S^+ and S^-. By the above argument, in a C^2 patch, the inflection occurs along the rule segment where $\frac{d\mathbf{Q}(t)}{dt} \cdot \mathbf{P} = 0$ is satisfied. Also, if the surface is not C^2, then it is on a rule segment. Therefore, if the S^- surface is bent in a different direction at $\lim_{t \to t_1^-} \mathbf{Y}_1(t)$ and $\lim_{t \to t_2^-} \mathbf{Y}_2(t_2)$, then a path from $\mathbf{Y}_1$ to $\mathbf{Y}_2$ must cross a rule segment. Because rule segments do not intersect, S^+ and S^- keep their own bending orientations. Therefore, the assignment for the semicrease is unchanged along the segment. □

By Lemma 6.6, we can define the bending direction of a rule segment: A developable uncreased surface bends mountain or valley at a rule segment if a relative interior point of the rule segment bends mountain or valley, respectively. Furthermore, because the frames are identical, we can define the principle curvature frame $(\mathbf{Q}, \mathbf{R}, \mathbf{P})$ of a rule segment by the principle curvature frame at any relative interior point on the rule segment.

6.3. Crease versus rule segment. Next we consider the mountain-valley relation between a rule segment and a crease.

First, consider a smoothly folded crease $\mathbf{X}$ with left and right surface *ruling vectors* $\mathbf{R}_L$ and $\mathbf{R}_R$, defined as unit vectors that lie along the rule segments on surfaces S_L and S_R incident to $\mathbf{X}$. (If there is a planar region incident to $\mathbf{X}$, these ruling vectors will not be unique.) A left-side ruling vector $\mathbf{R}_L$ lives in the plane perpendicular to $\mathbf{P}_L$. Therefore, the vector can be represented by

$$\mathbf{R}_L = (\cos\theta_L)\mathbf{T} + (\sin\theta_L)(\mathbf{P}_L \times \mathbf{T}),$$

where we call θ_L the *left-side ruling angle* of the ruling, which is nonzero by Lemma 4.6. Because the ruling angle is intrinsic, the ruling vector in 2D is represented by $\mathbf{r}_L = (\cos\theta_L)\mathbf{t} + (\sin\theta_L)\hat{\mathbf{b}}$. The orientation of the left-side ruling vector is chosen to orient to the left, i.e., $\mathbf{r}_L \cdot \hat{\mathbf{b}} > 0$, so θ_L is positive. Similarly, ruling vector $\mathbf{R}_R$ on the right surface is represented by $\mathbf{R}_R = (\cos\theta_R)\mathbf{T} - (\sin\theta_R)(\mathbf{P}_R \times \mathbf{T})$, using *right-side ruling angle* θ_R. The orientation is chosen to be on the right side, so $\theta_R > 0$.

Lemma 6.7. *Consider a uniquely ruled smoothly folded crease* $\mathbf{X}$ *with locally* C^2 *surfaces on both sides (no semicreases). Then, the rule segment on the left side of* $\mathbf{X}$ *bends valley if and only if* $\mathbf{N} \cdot \mathbf{P}_L > 0$. *Symmetrically, the surface bends valley on the right side if and only if* $\mathbf{N} \cdot \mathbf{P}_R > 0$.

Proof. Build the principle curvature frame $(\mathbf{Q}(t), \mathbf{R}(t), \mathbf{P}(t))$ of rule segment parameterized by the arclength t in the principle curvature direction. Consider corresponding point $\mathbf{X}(s)$ and the arclength parameter $s = s(t)$ along the crease at the rule segment parameterized by t. Because the surface is locally C^2 around the rule segment, $\frac{ds}{dt} > 0$. Because we consider the left side of the surface, $\mathbf{P}_L(s) = \mathbf{P}(t)$. Let θ be the angle between $\mathbf{R}(t)$ and $\mathbf{T}(s)$, i.e., $\mathbf{T}(s) = \sin\theta\mathbf{Q}(t) + \cos\theta\mathbf{R}(t)$. By Lemma 4.6, $0 < \theta < \pi$, and we get

$$\mathbf{Q} = (\csc\theta)\mathbf{T} - (\cot\theta)\mathbf{R}. \tag{6.1}$$

Assume that the surface bends valley at the rule segment, i.e.,

$$V(t) = \frac{d\mathbf{Q}(t)}{dt} \cdot \mathbf{P}(t) > 0. \tag{6.2}$$

Using orthogonality of vectors $\mathbf{Q}$ and $\mathbf{P}$, i.e., $\mathbf{Q}(t) \cdot \mathbf{P}(t) = 0$, and taking derivatives, we obtain

$$\frac{d\mathbf{Q}}{dt} \cdot \mathbf{P} + \mathbf{Q} \cdot \frac{d\mathbf{P}}{dt} = 0.$$

Then,

$$\begin{aligned} V(t) &= -\mathbf{Q} \cdot \frac{d\mathbf{P}}{dt} \\ &= -\Big((\csc\theta)\mathbf{T} - (\cot\theta)\mathbf{R}\Big) \cdot \frac{d\mathbf{P}}{dt} \\ &= -(\csc\theta)\mathbf{T} \cdot \frac{d\mathbf{P}}{dt}. \end{aligned}$$

Here, we used Equation (6.1). By the orthogonality of vectors $\mathbf{T}$ and $\mathbf{P}$, we get

$$\mathbf{T} \cdot \frac{d\mathbf{P}}{dt} = \frac{d\mathbf{T}}{dt} \cdot \mathbf{P}.$$

Then,

$$\begin{aligned} V(t) &= (\csc\theta)\frac{d\mathbf{T}(s)}{dt}\cdot\mathbf{P}(t) \\ &= (\csc\theta)\frac{ds}{dt}\frac{d\mathbf{T}(s)}{ds}\cdot\mathbf{P}(t) \\ &= (\csc\theta)\frac{ds}{dt}K(s)\mathbf{N}(s)\cdot\mathbf{P}_L(s). \end{aligned}$$

Because $\csc\theta > 0$, $\frac{ds}{dt} > 0$, and $K(s) > 0$, Equation (6.2) is equivalent to $\mathbf{N}(s)\cdot\mathbf{P}_L(s) > 0$. □

Now we make a stronger statement, allowing the ruling vectors to be not unique and the surfaces to be not C^2.

Corollary 6.8. *Consider a smoothly folded crease* $\mathbf{X}$. *Then, a rule segment on the left side of* $\mathbf{X}$ *bends valley if and only if* $\mathbf{N}\cdot\mathbf{P}_L > 0$. *Symmetrically, the surface bends valley on the right side if and only if* $\mathbf{N}\cdot\mathbf{P}_R > 0$.

Proof. Consider rule segments at $\mathbf{X}(\tilde{s})$. By Theorem 5.1, the crease is cone free, so a rule segment is either (1) between two C^2 ruled surfaces or (2) between a plane and a C^2 ruled surfaces.

Consider Case 1, and let S^- and S^+ be the two surfaces. Because there are no cone rulings, S^- and S^+ are locally formed by unique rulings emanating from $\mathbf{X}(s)$ at $s < \tilde{s}$ and $s > \tilde{s}$, respectively. Then,

$$\lim_{s\to\tilde{s}^-}\mathbf{N}(s)\cdot\mathbf{P}_L(s) = \lim_{s\to\tilde{s}^+}\mathbf{N}(s)\cdot\mathbf{P}_L(s) = \mathbf{N}(s)\cdot\mathbf{P}_L(s).$$

So, both surfaces S^- and S^+ bend valley if and only if $\mathbf{N}(s)\cdot\mathbf{P}_L(s) > 0$.

Next, consider Case 2. By symmetry, assume that S^- is planar and S^+ is a C^2 ruled surface. Then, S^+ is locally formed by unique rule segments emanating from $\mathbf{X}(s)$ at $s > \tilde{s}$. Hence, S^+, and thus the rule segment, bends valley if and only if $\mathbf{N}(s)\cdot\mathbf{P}_L(s) > 0$. □

Theorem 6.9. *Consider a smoothly folded curved crease* $\mathbf{X}$. *A rule segment incident to* $\mathbf{X}(\tilde{s})$ *on the convex side of* $\mathbf{X}(\tilde{s})$ *has the same mountain/valley assignment as the crease, while a rule segment incident to* $\mathbf{X}(\tilde{s})$ *on the concave side of* $\mathbf{X}(\tilde{s})$ *has the opposite mountain/valley assignment as the crease.*

Proof. Assume by symmetry that the left side of the paper is the convex side ($\hat{k}(s) < 0$). Also, assume that the crease is a valley, i.e., $(\hat{\mathbf{B}}\times\mathbf{P}_L)\cdot\mathbf{T} = (\mathbf{P}_L\times\mathbf{B})\cdot\mathbf{T} > 0$. Then, the top-side normal of the osculating plane is $\hat{\mathbf{B}} = -\mathbf{B}$, and thus $\hat{\mathbf{N}} = -\mathbf{N}$.

Now

$$\begin{aligned} (\mathbf{P}_L\times\mathbf{B})\cdot\mathbf{T} &= (\mathbf{P}_L\times(\mathbf{T}\times\mathbf{N}))\cdot\mathbf{T} \\ &= (\mathbf{T}(\mathbf{P}_L\cdot\mathbf{N}) - \mathbf{N}(\mathbf{P}_L\cdot\mathbf{T}))\cdot\mathbf{T} > 0. \end{aligned}$$

The second term disappears because $\mathbf{P}_L\cdot\mathbf{T} = 0$. Therefore, $\mathbf{P}_L\cdot\mathbf{N} > 0$, so the left side is valley. □

6.4. Creases connected by a rule segment. Now consider two creases connected by a rule segment. By Lemma 6.9, we get the following:

Corollary 6.10. *Consider two smoothly folded creases connected by a rule segment. If the rule segment is on the concave sides of both creases, or on the convex sides of both creases, then the creases must have the same direction (mountain or valley). If a rule*

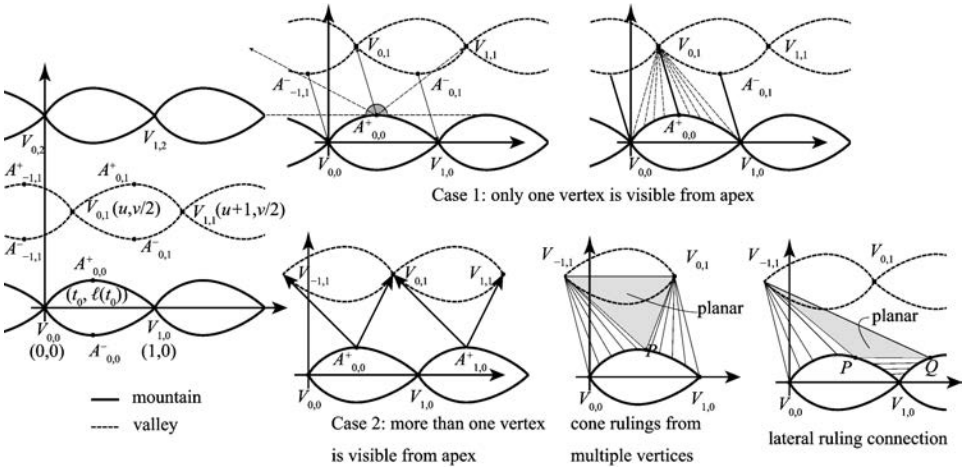

FIGURE 8. Ruling conditions for a lens tessellation.

segment is on the convex side of one crease and the concave side of the other crease, then the creases must have the opposite direction (one mountain and one valley).

7. Lens Tessellation

In this section, we use the qualitative properties of rulings obtained in previous sections to reconstruct rule segments from a crease pattern of the generalized version of lens tessellation.

First, as illustrated in Figure 8, we define the *lens tessellation* parameterized by a convex C^2 function $\ell : [0,1] \to [0,\infty)$ with $\ell(0) = \ell(1) = 0$, horizontal offset $u \in [0,1)$, and vertical offset $v \in (0,\infty)$, to consist of

(1) mountain creases $\gamma^{\pm}_{i,2j} = \{(t+i, \pm\ell(t) + jv) \mid t \in [0,1]\}$ for $i, j \in \mathbb{Z}$;

(2) valley creases $\gamma^{\pm}_{i,2j+1} = \{(1-t+i+u, \pm\ell(1-t) + (j+\frac{1}{2})v)\} \mid t \in [0,1]\}$ for $i, j \in \mathbb{Z}$.

Define the *vertices* to be points of the form $V_{i,2j} = (i, jv)$ and $V_{i,2j+1} = (i+u, (j+\frac{1}{2})v)$. Four creases meet at each vertex.

Because $\ell(t)$ is convex, it has a unique maximum $\ell(t^*)$ at some $t = t^*$. Define the *apex* $A_{i,k}$ of crease $\gamma^{\pm}_{i,k}$ to be the point of the crease at $t = t^*$, i.e., $A^{\pm}_{i,2j} = (t^* + i, \pm\ell(t^*) + jv)$ and $A^{\pm}_{i,2j+1} = (1 - t^* + i + u, \pm\ell(1-t^*) + (j+\frac{1}{2})v)$.

7.1. Necessary conditions. Consider a crease point $\mathbf{x}(s)$. A point $\mathbf{y}$ on the crease pattern (a vertex or crease point) is *visible* from $\mathbf{x}(s)$ on the left (right) side of $\mathbf{x}$ at $\mathbf{x}(s)$ if the oriented open line segment $\overrightarrow{\mathbf{x}(s)\mathbf{y}}$ is on the left (right) side of $\mathbf{x}(s)$ and does not share a point with the crease pattern. If $\mathbf{x}(s)$ and $\mathbf{y}$ are the endpoints of a rule segment, then certainly they must be visible from each other.

THEOREM 7.1. *A lens tessellation can smoothly fold only if there is a vertex $V_{i,1}$ visible from every point on crease $\gamma^{+}_{0,0}$ on the convex side.*

PROOF. Refer to Figure 8. By Corollary 4.7, there must be a rule segment emanating from $A^{+}_{0,0}$ on the convex side of $\gamma^{+}_{0,0}$. The other endpoint B of that rule segment must be visible from $A^{+}_{0,0}$ on the convex side of $\gamma^{+}_{0,0}$. Because the tangent line of $\gamma^{+}_{0,0}$ at $A^{+}_{0,0}$ is horizontal, any such visible point B must lie on the union of creases $\gamma^{-}_{i,1}$ and vertices $V_{i,1}$

for $i \in \mathbb{Z}$. By Theorem 6.10, B cannot be on the relative interior of one of the valley creases $\gamma^-_{i,1}$ because then the rule segment would be on the concave sides of creases of opposite direction. Thus, B must be among the vertices $V_{i,1}$ for $i \in \mathbb{Z}$.

First, consider the case that only one vertex $V_{n,1}$ is visible from $A^+_{0,0}$ on the convex side of $\gamma^+_{0,0}$. Then, $A^+_{0,0}V_{n,1}$ must be a rule segment. By symmetry, $V_{1,0}A^-_{n,1}$ is also a rule segment. Consider a point on $\gamma^+_{0,0}$ between $A^+_{0,0}$ and $V_{0,1}$, which by Corollary 4.7 has a rule segment on the positive side of $\gamma^+_{0,0}$. This rule segment cannot cross the existing rule segments $A^+_{0,0}V_{n,1}$ and $V_{1,0}A^-_{n,1}$, so its other endpoint must be $V_{n,1}$, $A^-_{n,1}$, or between $V_{n,1}$ and $A^-_{n,1}$ on curve $\gamma^-_{n,1}$. By Theorem 6.10, the only possible ruling is to have a cone apex at $V_{n,1}$. Similarly, rule segments from points between $V_{0,0}$ and $A^+_{0,0}$ on $\gamma^+_{0,0}$ must end at $V_{n,1}$. Therefore, $V_{n,1}$ is visible from every point on crease $\gamma^+_{0,0}$ on the convex side.

Second, consider the case in which more than one vertex $V_{i,1}$ is visible from apex $A^+_{0,0}$ on the convex side of $\gamma^+_{0,0}$. Suppose for contradiction that there is no common vertex visible from the entire curve $\gamma^+_{0,0}$. Similar to the previous case, there must be a rule segment from apex $A^+_{0,0}$ to one of the vertices $V_{n,1}$. But, we assumed that some other point of $\gamma^+_{0,0}$ cannot see $V_{n,1}$. By symmetry, suppose that point is to the right of $A^+_{0,0}$. There is a transition point P on the relative interior of $\gamma^+_{0,0}$ when the endpoints of rulings change from $V_{n,1}$ to either (a) another vertex $V_{m,1}$ with $m > n$ or (b) a point on $\gamma^+_{1,0}$. (See Figure 8.) At such a point P, we have two rule segments. By Theorem 5.1, P cannot be a cone apex. Hence, there must be a planar region between the two rule segments. Specifically, in case (a), the triangle $PV_{n,1}V_{m,1}$ is planar, which contains all of $\gamma^-_{n,1}$, contradicting that the folded piece of paper is not C^1 on $\gamma^-_{n,1}$. In case (b), let Q be the point on $\gamma^+_{1,0}$. The triangle $PQV_{n,1}$ is planar. This triangle cannot intersect $\gamma^-_{n,1}$, because the folded piece of paper is not C^1 on $\gamma^-_{n,1}$. In particular, the curve $\gamma^-_{n,1}$ cannot intersect the segment $V_{n,1}V_{0,1}$ (which begins in the triangle). Because $\gamma^+_{1,0}$ is a 180° rotation of $\gamma^-_{n,1}$ mapping $V_{n,1}$ to $V_{0,1}$, we symmetrically have that the curve $\gamma^+_{1,0}$ cannot intersect the same segment $V_{n,1}V_{0,1}$. Thus, this segment is a visibility segment, as is $V_{n,1}V_{0,0}$. By convexity of the lens, $V_{n,1}$ can see the entire curve $\gamma^+_{1,0}$. Therefore, there is in fact a common vertex visible from the curve $\gamma^+_{0,0}$. □

7.2. Existence and sufficiency. Finally we prove that the condition from Theorem 7.1 is also sufficient:

THEOREM 7.2. *A lens tessellation can fold smoothly if there is a vertex $V_{i,1}$ visible from every point on crease $\gamma^+_{0,0}$ on the convex side.*

PROOF. First, we construct the folding of one "gadget," $(i, j) = 0$; refer to Figure 9. We can add an integer to u to assume that $V_{0,1}$ is the visible vertex from apex $A^+_{0,0}$. In 2D, this gadget is bounded by a quadrangle of rule segments with vertex coordinates $V_{0,0} = (0, 0)$, $V_{0,-1} = (u, -\frac{1}{2}v)$, $V_{1,0} = (1, 0)$, and $V_{0,1} = (u, \frac{1}{2}v)$. This kite module is decomposed by its creases into an upper wing part U, middle lens part M, and lower wing part L. We assume that M is ruled parallel to the y-axis: The rule segments of M are of the form $(t, \ell(t))$ and $(t, -\ell(t))$ parameterized by t. (We can make this assumption because we are constructing a folded state.) We also assume that U consists of cone rulings between $V_{0,1}$ and $(t, \ell(t))$ while L consists of cone rulings between $V_{0,-1}$ and $(t, -\ell(t))$ using the same parameter t.

The folding $f(M)$ is a cylindrical surface with parallel rulings. We orient the folded form such that this ruling direction is parallel to the y-axis and $\overrightarrow{f(V_{0,0})f(V_{1,0})}$ is parallel to the positive direction of the x-axis. Then, the orthogonal projection of $f(M)$ to the xz-plane is a curve γ, and a ruling at t on M corresponds to a point on $\gamma(t)$ while t is the arclength parameter.

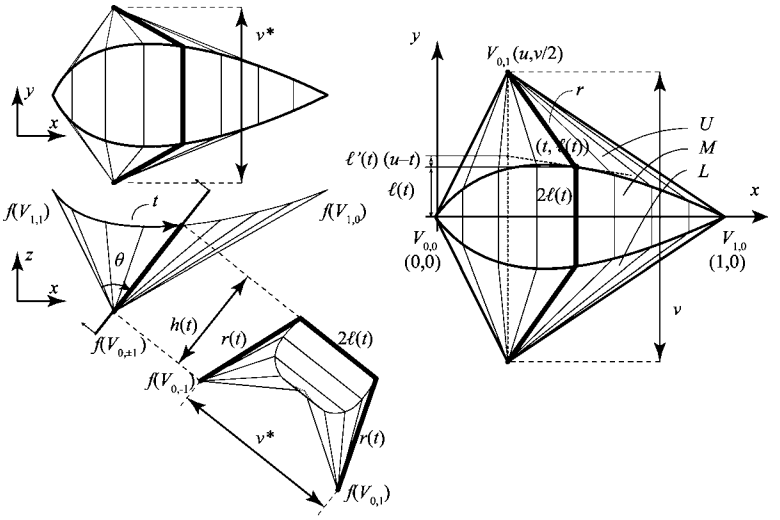

FIGURE 9. A modular kite structure.

We further assume that the folded state is symmetric with respect to reflection through a plane passing through $\overrightarrow{f(V_{0,0})f(V_{1,0})}$ and parallel to the xz-plane. Let the distance between $f(V_{0,-1})$ and $f(V_{0,1})$ be denoted by v^*, where $0 < v^* < v$. We will show that there is a valid folded state for arbitrary v^* if it is sufficiently close to v.

Consider the set of rule segments of U, M, and L at parameter t and its folding. Then, by our symmetry assumption, these segments form a planar polyline that, together with segments $f(V_{0,-1})$ and $f(V_{0,1})$, forms an isosceles trapezoid with base length v^* and top length $2\ell(t)$. The legs are the length of the rule segments, which can be calculated from the crease pattern as $r(t) = \sqrt{(u-t)^2 + (v/2 - \ell(t))^2}$. Such a trapezoid exists because $0 < v^* < v \le 2\ell(t) + 2r(t)$. The height of the trapezoid $h(t)$ is given by

$$h(t) = \sqrt{(v - v^*)\left(\frac{v + v^*}{4} - \ell(t)\right) + (t-u)^2}.$$

Now consider the projection of this trapezoid in the xz-plane. This projection is a line segment between two points, namely the projections of $V_{0,1}$ and $\gamma(t)$, and it must have length of $h(t)$. We use the following lemma to solve for γ:

LEMMA 7.3. *If an arclength-parameterized crease* $\mathbf{x}(s)$ *has unique rule segments on one side incident to cone apex* $\mathbf{a}$*, then an embedding* $\mathbf{f}$ *is a proper folding if and only if folded curve* $\mathbf{X} = \mathbf{f} \circ \mathbf{x}$ *is also arclength parameterized, and rule segments from* $\mathbf{a}$ *to* $\mathbf{x}(s)$ *map isometrically to rule segments from* $\mathbf{A}$ *to* $\mathbf{X}(s)$*, where* $\mathbf{A} = \mathbf{f} \circ \mathbf{a}$*.*

PROOF. Necessity ("only if" part) is obvious, so we prove sufficiency ("if" part). The folded curve is arclength parameterized by s as $\frac{d\mathbf{X}(s)}{ds} = \frac{d\mathbf{x}(s)}{ds} = 1$, and the length of ruling segment $L(s)$ must equal $L(s) = \|\mathbf{x}(s) - \mathbf{a}\| = \|\mathbf{X}(s) - \mathbf{A}\|$. Let $\mathbf{r}(s)$ denote the unit ruling vectors from the apex toward the curve in 2D, i.e., $\mathbf{r}(s) = (\mathbf{x}(s) - \mathbf{a})/L(s)$. Similarly denote the unit ruling vector in 3D by $\mathbf{R}(s) = (\mathbf{X}(s) - \mathbf{A})/L(s)$. Consider a coordinate system using arclength s and radius ℓ. The conical portion of the face formed by the crease and a point is uniquely ruled at any point, so (s, ℓ) uniquely represent a point on the portion. A point (s, ℓ) in 2D corresponds to $\mathbf{a} + \ell\mathbf{r}(s)$, which is mapped to 3D to $\mathbf{A} + \ell\mathbf{R}(s)$. Consider a 2D

C^1 curve $\mathbf{y}(t)$ represented by $(s(t), \ell(t))$, where t is the arclength parameterization. Then, the total derivative of $\mathbf{y}(t) = \mathbf{a} + \ell(t)\mathbf{r}(s(t))$ is

$$\frac{d\mathbf{y}}{dt} = \frac{\partial \mathbf{y}}{\partial s}\frac{ds}{dt} + \frac{\partial \mathbf{y}}{\partial \ell}\frac{d\ell}{dt} = \ell \frac{d\mathbf{r}}{ds}\frac{ds}{dt} + \mathbf{r}\frac{d\ell}{dt}.$$

Then, by taking the dot product with itself,

$$\begin{aligned}\left\|\frac{d\mathbf{y}}{dt}\right\|^2 = & \quad \ell^2 \left\|\frac{d\mathbf{r}}{ds}\right\|^2 \left(\frac{ds}{dt}\right)^2 + 2\ell \frac{d\mathbf{r}}{ds}\cdot\mathbf{r}\left(\frac{ds}{dt}\right)\left(\frac{d\ell}{dt}\right) + \|\mathbf{r}\|^2\left(\frac{d\ell}{dt}\right)^2 \\ = & \quad \ell^2 \left\|\frac{d\mathbf{r}}{ds}\right\|^2 \left(\frac{ds}{dt}\right)^2 + \left(\frac{d\ell}{dt}\right)^2,\end{aligned}$$

where we used $\mathbf{r}\cdot\mathbf{r} = 1$ and $2\frac{d\mathbf{r}}{ds}\cdot\mathbf{r} = \frac{d}{ds}(\mathbf{r}\cdot\mathbf{r}) = 0$. Because $L(s)\mathbf{r}(s) = \mathbf{x}(s) - \mathbf{a}$, taking derivatives yields

$$L\frac{d\mathbf{r}}{ds} + \frac{dL}{ds}\mathbf{r} = \frac{d\mathbf{x}}{ds}.$$

By taking the dot product,

$$L^2\left\|\frac{d\mathbf{r}}{ds}\right\|^2 + \left(\frac{dL}{ds}\right)^2 = \left\|\frac{d\mathbf{x}}{ds}\right\|^2 = 1,$$

again using $\frac{d\mathbf{r}}{ds}\cdot\mathbf{r} = 0$ and $\mathbf{r}\cdot\mathbf{r} = 1$. Thus,

$$\left\|\frac{d\mathbf{y}}{dt}\right\|^2 = \frac{\ell^2}{L^2}\left(1 - \left(\frac{dL}{ds}\right)^2\right)\left(\frac{ds}{dt}\right)^2 + \left(\frac{d\ell}{dt}\right)^2.$$

The mapped crease $\mathbf{Y}(t)$ in 3D is defined by $\mathbf{Y}(t) = \mathbf{A} + \ell(t)\mathbf{R}(s(t))$. Then,

$$\left\|\frac{d\mathbf{Y}}{dt}\right\|^2 = \frac{\ell^2}{L^2}\left(1 - \left(\frac{dL}{ds}\right)^2\right)\left(\frac{ds}{dt}\right)^2 + \left(\frac{d\ell}{dt}\right)^2,$$

similarly using $\mathbf{R}\cdot\mathbf{R} = 1$, $\frac{d\mathbf{R}}{ds}\cdot\mathbf{R} = 0$, and $\left\|\frac{d\mathbf{X}}{ds}\right\|^2 = 1$. Therefore, $\left\|\frac{d\mathbf{y}}{dt}\right\|^2 = \left\|\frac{d\mathbf{Y}}{dt}\right\|^2 = 1$ and the mapping is isometric. □

A similar argument works for cylindrical surfaces.

LEMMA 7.4. *If an arclength-parameterized crease* $\mathbf{x}(s)$ *has unique rule segments on one side parallel to* $\mathbf{r}$*, such that* $\mathbf{r}$ *is perpendicular to segment c, then an embedding* $\mathbf{f}$ *is a proper folding if and only if folded curve* $\mathbf{X} = \mathbf{f}\circ\mathbf{x}$ *is also arclength parameterized, and the perpendicular rule segments from* $\mathbf{x}(s)$ *to c map isometrically to rule segments from* $\mathbf{X}(s)$ *perpendicularly to a planar curve C, where* $C = \mathbf{f}\circ c$*.*

PROOF. Necessity ("only if" part) is obvious, so we prove sufficiency ("if" part). The folded curve is arclength parameterized by s as $\frac{d\mathbf{X}(s)}{ds} = \frac{d\mathbf{x}(s)}{ds} = 1$, and the length of ruling segment $L(s)$ must equal $L(s) = \|\mathbf{x}(s) - \mathbf{c}(s)\| = \|\mathbf{X}(s) - \mathbf{C}(s)\|$. Let $\mathbf{r}$ denote the unit ruling vectors from the apex toward the curve in 2D, i.e., $\mathbf{x}(s) = \mathbf{c}(s) + L(s)\mathbf{r}$. Similarly denote the unit ruling vector in 3D by $\mathbf{X}(s) = \mathbf{C}(s) + L(s)\mathbf{R}$. Consider a coordinate system using arclength s and length along the ruled segments ℓ. The face is uniquely ruled between the crease and the curve at any point, so (s, ℓ) uniquely represent a point on the portion. A point (s, ℓ) in 2D corresponds to $\mathbf{c}(s) + \ell\mathbf{r}$, which is mapped to 3D to $\mathbf{C}(s) + \ell\mathbf{R}$. Consider a 2D C^1 curve $\mathbf{y}(t)$ represented by $(s(t), \ell(t))$, where t is the arclength parameterization. Then, the total derivative of $\mathbf{y}(t) = \mathbf{c}(s) + \ell(t)\mathbf{r}$ is

$$\frac{d\mathbf{y}}{dt} = \frac{\partial \mathbf{y}}{\partial s}\frac{ds}{dt} + \frac{\partial \mathbf{y}}{\partial \ell}\frac{d\ell}{dt} = \frac{d\mathbf{c}}{ds}\frac{ds}{dt} + \mathbf{r}\frac{d\ell}{dt}.$$

Then,

$$\left\|\frac{d\mathbf{y}}{dt}\right\|^2 = \left\|\frac{d\mathbf{c}}{ds}\right\|^2\left(\frac{ds}{dt}\right)^2 + 2\frac{d\mathbf{c}}{ds}\cdot\mathbf{r}\left(\frac{ds}{dt}\right)\left(\frac{d\ell}{dt}\right) + \|\mathbf{r}\|^2\left(\frac{d\ell}{dt}\right)^2$$
$$= \left\|\frac{d\mathbf{c}}{ds}\right\|^2\left(\frac{ds}{dt}\right)^2 + \left(\frac{d\ell}{dt}\right)^2,$$

where we used $\mathbf{r}\cdot\mathbf{r} = 1$ and $\frac{d\mathbf{c}(s)}{ds}\cdot\mathbf{r} = 0$. Now differentiate $L(s)\mathbf{r} + \mathbf{c}(s) = \mathbf{x}(s)$ to obtain

$$\frac{d\mathbf{c}}{ds} + \frac{dL}{ds}\mathbf{r} = \frac{d\mathbf{x}}{ds}.$$

By taking the dot product,

$$\left\|\frac{d\mathbf{c}}{ds}\right\|^2 + \left(\frac{dL}{ds}\right)^2 = \left\|\frac{d\mathbf{x}}{ds}\right\|^2 = 1,$$

again using $\frac{d\mathbf{c}}{ds}\cdot\mathbf{r} = 0$ and $\mathbf{r}\cdot\mathbf{r} = 1$. Thus,

$$\left\|\frac{d\mathbf{y}}{dt}\right\|^2 = \left(1 - \left(\frac{dL}{ds}\right)^2\right)\left(\frac{ds}{dt}\right)^2 + \left(\frac{d\ell}{dt}\right)^2.$$

The mapped crease $\mathbf{Y}(t)$ in 3D is defined by $\mathbf{Y}(t) = \mathbf{C}(s) + \ell(t)\mathbf{R}$. Then,

$$\left\|\frac{d\mathbf{Y}}{dt}\right\|^2 = \left(1 - \left(\frac{dL}{ds}\right)^2\right)\left(\frac{ds}{dt}\right)^2 + \left(\frac{d\ell}{dt}\right)^2,$$

similarly using $\mathbf{R}\cdot\mathbf{R} = 1$, $\frac{d\mathbf{C}}{ds}\cdot\mathbf{R} = 0$, and $\left\|\frac{d\mathbf{X}}{ds}\right\|^2 = 1$. Therefore, $\left\|\frac{d\mathbf{y}}{dt}\right\|^2 = \left\|\frac{d\mathbf{Y}}{dt}\right\|^2 = 1$ and the mapping is isometric. □

By Lemmas 7.3 and 7.4, the existence of the folded form is ensured by constructing the folded crease $f(\gamma)$ such that, in the folded state, the distance between $V_{0,1}$ and $f(\gamma(t))$ is always $r(t)$ and the distance from the xz-plane is always $\ell(t)$. If we view the projection of the curve, this is equivalent to constructing a curve represented by polar coordinate $(\theta(t), h(t))$ $(\theta \in \mathbb{R})$ such that (i) the curve has arclength t and (ii) $\theta(t)$ is a monotonic function (in order to avoid self-intersection). Condition (i) yields a differential equation:

$$1 = h^2\left(\frac{d\theta(t)}{dt}\right)^2 + h'(t)^2.$$

Condition (ii) gives us $0 < \frac{d\theta(t)}{dt}$ and $h(t) > 0$, so the differential equation becomes

$$\frac{d\theta(t)}{dt} = \frac{1}{h(t)}\sqrt{1 - \left(\frac{dh(t)}{dt}\right)^2},$$

which has solution

$$\theta(t) = \int_0^t \frac{1}{h(t)}\sqrt{1 - \left(\frac{dh(t)}{dt}\right)^2}\,dt$$

if and only if $(\frac{dh(t)}{dt})^2 \le 1$ for $t \in (0, 1)$. Combined with condition (ii), $(\frac{dh(t)}{dt})^2 < 1$, and

$$\left(\frac{dh(t)}{dt}\right)^2 = \frac{\left[(t-u) - \frac{1}{2}(v - v^*)\ell'(t)\right]^2}{(t-u)^2 + (v - v^*)\left[\frac{1}{4}(v + v^*) - \ell(t)\right]} < 1,$$

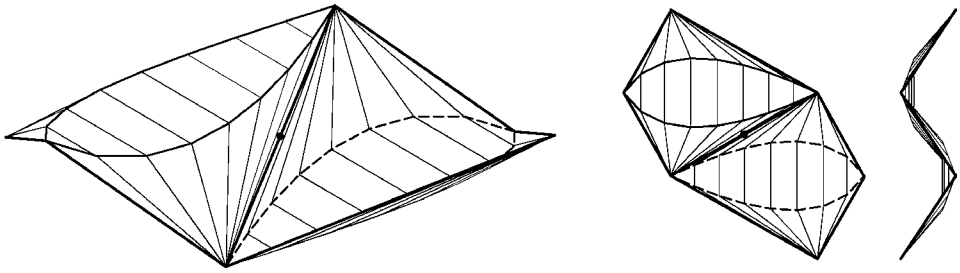

FIGURE 10. The connection of kite structures.

which is equivalent to

$$-\frac{1}{4}(v-v^*)\left[1+\left(\frac{d\ell(t)}{dt}\right)^2\right]+\left[\frac{1}{2}v-\left(\ell(t)+\frac{d\ell(t)}{dt}(u-t)\right)\right]>0.$$

Because $\ell(t)+\frac{d\ell(t)}{dt}(u-t)$ represents the y-coordinate of the intersection between the tangent line to $\gamma^+_{0,0}$ at t and a vertical line passing through $V_{0,1}$, $\frac{v}{2}-(\ell(t)+\frac{d\ell(t)}{dt}(u-t))$ is always positive. Also, $1+(\frac{d\ell(t)}{dt})^2$ is positive, so the condition is given by

$$v-v^*<\frac{4\left[\frac{v}{2}-\left(\ell(t)+\frac{d\ell(t)}{dt}(u-t)\right)\right]}{1+\left(\frac{d\ell(t)}{dt}\right)^2}.$$

If we define $v^*_{lim}<v$ as

$$v-v^*_{lim}=4\left[\frac{v}{2}-\left(\ell(t)+\frac{d\ell(t)}{dt}(u-t)\right)\right]\Big/\left[1+\left(\frac{d\ell(t)}{dt}\right)^2\right],$$

then there exists a continuous solution for v^* in (v^*_{lim},v).

Now that we have folded an individual gadget, we can tile the gadget to get a proper folding of the overall crease pattern. Here, we use the fact that the oriented folded module, for a sufficiently small fold angle, projects to a kite in the xy-plane.

Consider inversions of the oriented folded module through the midpoints of its boundary edges, followed by negating all normals to swap the top and bottom sides of the paper (Figure 10). If we consider the xy-projection, the operation corresponds to 180° rotation around the midpoint of the kite, resulting in a tessellation. Thus, in particular, there are no collisions between the copies of the folded module. Because each connecting edge is mapped onto itself in 3D, this tessellation has no gaps in 3D. Also, because the boundary is on a ruled segment, the surface normal vector is constant along each edge. The surface normal is flipped by the inversion and then negated back to its original vector, so the surface normals at corresponding points match. Thus, the shared boundaries remain uncreased in the tessellated folding. To show that this tessellated folding comes from one sheet of paper, we can apply the same tiling transformation to the crease-pattern module, which is also a kite, so it tiles the plane with the same topology and intrinsic geometry. Therefore, the plane can fold into the infinitely tiled folding. □

8. Conclusion

We still have a long way to go to obtain a general theory of curved creases. Nonetheless, we hope that the tools built in this work will enable the design and analysis of more

curved-crease origami models and will serve as a useful foundation to build up the underlying mathematics.

Acknowledgments

We thank the Huffman family for access to the third author's work and permission to continue in his name.

References

[Demaine and O'Rourke 07] Erik D. Demaine and Joseph O'Rourke. *Geometric Folding Algorithms: Linkages, Origami, Polyhedra*. Cambridge, UK: Cambridge University Press, 2007. MR2354878 (2008g:52001)

[Demaine et al. 11] Erik D. Demaine, Martin L. Demaine, Vi Hart, Gregory N. Price, and Tomohiro Tachi. "(Non)existence of Pleated Folds: How Paper Folds between Creases." *Graphs and Combinatorics* 27:3 (2011), 377–397. MR2787424 (2012i:52030)

[Fuchs and Tabachnikov 99] Dmitry Fuchs and Serge Tabachnikov. "More on Paperfolding." *The American Mathematical Monthly* 106:1 (1999), 27–35. MR1674137 (99m:53009)

[Fuchs and Tabachnikov 07] Dmitry Fuchs and Serge Tabachnikov. "Developable Surfaces." In *Mathematical Omnibus: Thirty Lectures on Classic Mathematics*, Chapter 4. Providence: American Mathematical Society, 2007. MR2350979 (2008h:00002)

[Huffman 76] David A. Huffman. "Curvature and Creases: A Primer on Paper." *IEEE Transactions on Computers* C-25:10 (1976), 1010–1019.

MIT Computer Science and Artificial Intelligence Lab., Cambridge, Massachusetts
E-mail address: edemaine@mit.edu

MIT Computer Science and Artificial Intelligence Lab., Cambridge, Massachusetts
E-mail address: mdemaine@mit.edu

Department of Computer Science, University of California, Santa Cruz, California

School of Architecture, Pratt Institute, Brooklyn, New York
E-mail address: duks@pratt.edu

Department of General Systems Studies, The University of Tokyo, Japan
E-mail address: tachi@idea.c.u-tokyo.ac.jp